

# Pickering Emulsions Stabilized by Halloysite Nanotubes: From General Aspects to Technological Applications

Lorenzo Lisuzzo, Giuseppe Cavallaro, Stefana Milioto, and Giuseppe Lazzara\*

Besides surfactants, which decrease the interfacial tension between two immiscible liquids, also interfacially active particles can successfully stabilize an emulsion system by attaching at the liquid–liquid interface. The preparation of the resulting Pickering emulsions has been so far investigated starting from the study of the interactions arising between the dispersed droplets and the stabilizers, till the application of these systems in a wide range of different fields. This work is intended to provide an overall overview about the development of Pickering emulsions by considering the most general aspects and scanning the diverse types of solid stabilizers. Among them, Halloysite nanotubes play a major role as naturally derived clay with emulsifying capability owing to their cheap, abundant, green and biocompatible properties. Therefore, the design of Halloysite stabilized Pickering emulsions is the main content of this review, which will survey the role of nanotubes in providing colloidal stability and will comprehensively sum up the use of these particles in technological and industrial purposes: from environmental to catalytic, from health to cultural heritage related applications.

industrial or personal uses can increase environmental pollution (e.g., water contamination or CO<sub>2</sub> production) and can also lead to adverse health effects (e.g., irritation, allergic reactions or hemolytic issues).<sup>[6]</sup> Hence, an eco-friendly and sustainable alternative had to be found.

Pickering emulsions, which are named after the scientist who firstly reported about them, are characterized by the presence of interfacially active particles which provide stability.<sup>[7]</sup> These Pickering stabilizers adsorb at the oil/water interface, in the case of an oil-in-water or an water-in-oil emulsion, and play their role.<sup>[8]</sup> In particular, unlike conventional surfactants stabilized systems, the high colloidal stability has not to be found in the decrease of the surface tension but in the formation of a physical barrier at the interface.<sup>[9]</sup> The irreversible anchoring of (nano)particles can be explained by taking into account

the high energy needed for their desorption from the interface of the two immiscible liquids.<sup>[10]</sup> Hence, a strong steric barrier is created and the emulsions possess a high resistance to coalescence, deformation and Ostwald ripening with an effective protection of the droplet for a long time.<sup>[6]</sup>

Although the design of Pickering emulsions did not immediately receive much attention at the very beginning due to the lack of knowledge and to the limited choice of stabilizers, the recent advances of nanotechnology and material science provided a favorable scenario for their development on a large scale.<sup>[11]</sup> The several advantages of Pickering emulsions compared with surfactants stabilized droplets (e.g., reduced or no toxicity, low cost of production, easy storage, simple recovery) are the basis for their use in a wide range of different applications nowadays, ranging from food science to cosmetics, from oil recovery to catalysis and to drug delivery.<sup>[12–14]</sup> Many factors can affect the Pickering emulsions system. For instance, the chemical nature of the stabilizing particles, their shape and size but also their concentration and charge, the type of oil used during the preparation, the interactions arising between the counterparts, the pH of the medium, etc.<sup>[14]</sup>


As a consequence, the investigation of nanoclays based Pickering emulsions has become a major topic in material science and nanotechnology due to the wide choice of starting raw materials, each one possessing its peculiar features. In this paper, we will firstly focus on the general aspects and physico-chemical insights of Pickering systems. Then, the different particles which are mainly used for their design will be concisely considered. More interestingly, this review wants to sum up the recent advances in nanoclay-based Pickering emulsions with a

## 1. Introduction

Since the pioneering studies of Ramsden and Pickering in the early years of the last century, particles stabilized emulsions have been fascinating the scientific and academic community.<sup>[1,2]</sup> It is well known that an emulsion is a thermodynamically unstable system composed of two immiscible liquids where one is dispersed in the other.<sup>[3]</sup> Due to the high surface energy between the two immiscible phases, the droplets tend to coalesce until their complete separation.<sup>[4]</sup>

To prevent their breaking, conventional emulsions are generally stabilized by the addition of surfactants which can form a molecular film around the droplets and decrease the interfacial tension.<sup>[5]</sup> However, their utilization can cause some detrimental effects. The large-scale application of surfactants for

L. Lisuzzo, G. Cavallaro, S. Milioto, G. Lazzara  
Dipartimento di Fisica e Chimica  
Università degli Studi di Palermo  
Viale delle Scienze, pad. 17, Palermo 90128, Italy  
E-mail: giuseppe.lazzara@unipa.it

 The ORCID identification number(s) for the author(s) of this article can be found under <https://doi.org/10.1002/admi.202102346>.

© 2022 The Authors. Advanced Materials Interfaces published by Wiley-VCH GmbH. This is an open access article under the terms of the Creative Commons Attribution License, which permits use, distribution and reproduction in any medium, provided the original work is properly cited.

DOI: 10.1002/admi.202102346

special focus on Halloysite Nanotubes by reporting their development and also surveying the different fields of applications, which will be the main object of our attention here.

## 2. Pickering Emulsions: A General Overview

### 2.1. Adsorption of Pickering Stabilizers at the Interface: Physico-Chemical Insights

The formation of Pickering emulsions is the result of many factors which play a specific role in the emulsification mechanism.

Binks et al. reported that the energy needed for a spherical particle to be desorbed from the oil/water interface, namely the detachment energy ( $\Delta E_{\text{det}}$ ), can be described as:<sup>[15]</sup>

$$\Delta E_{\text{det}} = \pi r^2 \gamma_{\text{o/w}} (1 \pm |\cos \theta|)^2 \quad (1)$$

where  $r$  is the radius of the spherical particle,  $\gamma_{\text{o/w}}$  is the interfacial tension between oil and water,  $\theta$  is the three-phase contact angle (also known as the wetting contact angle). The “+” refers to desorption to the oil phase whereas the “-” refers to desorption to the water phase.

It is clear that the dimension of the adsorbing particles, the interfacial tension of the emulsion and the wettability are crucial parameters governing the stabilization of the Pickering system, as aforementioned.

In particular, the solid particles should attach at the oil/water interface being partially wetted by the two liquids and the magnitude of the contact angle determines the type of emulsion, either oil-in-water or water-in-oil (Figure 1).<sup>[16]</sup> Hydrophilic particles ( $\theta < 90^\circ$ ) preferentially form O/W emulsions while hydrophobic particles ( $\theta > 90^\circ$ ) tend to stabilize W/O droplets in the case of a single layer. When the Pickering emulsions are stabilized by multiple layers, instead, the values of contact angle fall within  $15^\circ < \theta < 120^\circ$  for O/W and  $50.7^\circ < \theta < 160^\circ$  for W/O emulsions, respectively.<sup>[17]</sup>

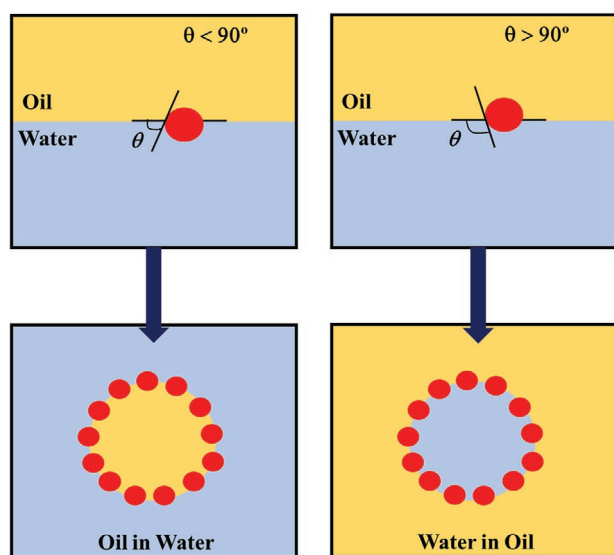


**Figure 1.** Scheme representing the relationship between the particles contact angle and the type of Pickering emulsions (O/W or W/O).

From Equation (1) one can see that also the dimensions of particles control the stability in terms of detachment energy. Indeed,  $\Delta E_{\text{det}}$  increases with the square of the sphere radius so that larger particles provide higher stabilization. However, Li et al. suggested that an upper limit must be considered to avoid sedimentation and to oppose the decrease of the adsorption kinetics, the result of which would be a less efficient packing at the liquid–liquid interface, as observed for extensively large starch particles used as stabilizers with no droplets formation.<sup>[18,19]</sup> On the opposite side, a lower limit is also required to reach a significant value of  $\Delta E_{\text{det}}$  and to avoid the Brownian effects to become significant enough to prevent the attachment of particles at the liquid–liquid interface.<sup>[20]</sup> As a general hypothesis, the diameter of a spherical stabilizing particle should be in the order of some micrometers to be irreversibly adsorbed, being the ratio between the detachment energy and the thermal energy ( $\Delta E_{\text{det}}/k_{\text{b}}T$ )  $\cong 10^7$ .<sup>[21]</sup>

This is in contrast with conventional emulsions, where surfactants constantly adsorb and desorb from the interface.<sup>[22]</sup> While in the latter case the stabilization is attributed to the variation of the interfacial tension, Pickering emulsions are irreversibly covered by solid particles that provide steric hindrance, thus avoiding coalesce upon droplets collision.<sup>[23,24]</sup>

Besides, the rheological variations and the increase of viscosity due to the presence of solids also contribute to the stability enhancement.<sup>[25–27]</sup> As a direct consequence, it was reported that the concentration of the active solids can affect the stability of Pickering emulsions. It can be intuitively noted that, as long as the concentration increases, a thicker layer is formed around each droplet and it slows down the coalescence rate while increasing the viscosity of the system.<sup>[28]</sup>

Besides being partially wetted by both the immiscible liquids without dissolving and besides the careful control of the particles dimensions needed to reach the formation of Pickering emulsions, the surface charge of Pickering stabilizers also plays a proper major role. The magnitude of the surface charge can be measured through  $\zeta$ -potential experiments. This parameter is crucial because it directly affects the adsorption of the solids and the interface. In particular, the particles tend to repel each other when the surface charge is very high and their attachment onto the droplet surface cannot occur.<sup>[29]</sup> Contrarily to it, a low surface charge promotes the coalescence and aggregation of particles at the interface, thus increasing the stability of the final emulsions system.<sup>[29]</sup>

It is worth to note that electrostatic attractions between the solid particles and the droplet surface with opposite charge could also be involved.<sup>[30]</sup> In light of these aspects, the environmental conditions must be considered because they can be tailored to adjust and optimize the surface charges. Any variations of pH or ionic strength could alter the electrostatic interactions through protonation/deprotonation of functional groups and also through screening effects created by the presence of electrolytes in the surrounding proximity of the interface.<sup>[31]</sup>

As described in Equation (1) the interfacial tension between oil and water holds a certain importance in the resulting adsorption mechanism although the system stability is not related to its direct reduction. Nonetheless, it was reported that the nature of the continuous and dispersed liquid phases determines the microstructure of the emulsions.<sup>[32]</sup> For instance, the different polarity, hydrophobicity and chemistry of functional groups in the

oil phase can considerably change the interfacial energy and the droplet interactions with the Pickering stabilizers, thus affecting the strength of attachment and the final stability.<sup>[33]</sup> More interestingly, the volume fractions of the two liquids should also be considered because they define the final surface that will be covered by the solid particles.<sup>[34]</sup> Literature reports that the ratio between the two phases influences the stability, the size and the type of emulsions, which showed an inversion (from oil-in-water to water-in-oil or vice versa) at a characteristic oil fraction value.<sup>[35]</sup>

It should be now clear that different parameters must be taken into account for the proper design of stable Pickering emulsions, each of them providing its specific contribution. Hence, the great interest for these systems arose and developed till nowadays.

## 2.2. What Kind of Particles Can Act as Pickering Emulsifiers?

The different factors affecting the formation of Pickering emulsions and their stability were debated by a general perspective in the previous paragraph. Until here, we referred to the interfacially active particles adsorbing at the liquid–liquid interface as “Pickering particles”, “Pickering stabilizers”, or simply as “solids”. However, a broad class of materials can be used for this purpose, depending on the final application for which the system has been thought: cosmetics, pharmaceutical formulations, food coatings, paints, catalysis, environmental remediation, etc. Herein, we will try to provide a clear overview of these materials.

Owing to their manageability and high colloidal stability, inorganic particles have been explored from the very beginning for the preparation of Pickering emulsions. To give an example, calcium carbonate (CaCO<sub>3</sub>) was employed for the droplets stabilization by Komatsu et al., and furtherly used to create templated inorganic capsules which are soluble in acidic media.<sup>[36]</sup> Metal oxides such as titania (TiO<sub>2</sub>) and magnetite (Fe<sub>3</sub>O<sub>4</sub>) were exploited with the aim to provide the stabilized Pickering emulsions with photocatalytic functionalities and magnetic-responsive performance.<sup>[37,38]</sup> For instance, the emulsions can be reversibly switched between stable and unstable states by mean of redox reactions or by applying external magnetic field and they can be used as extraction systems for purifying aqueous solutions with high efficiency.<sup>[39]</sup> Literature also reports the preparation of nanoceria (CeO<sub>2</sub>) stabilized Pickering emulsions for the design of nanocomposites possessing transparency in the visible region combined with a strong UV absorption, which is desired for UV-blocking coating applications.<sup>[40]</sup> Liu et al. developed black plasmonic colloidosomes by an emulsion-templating method where gold nanoparticles (AuNPs) were firstly used as Pickering stabilizers.<sup>[41]</sup> Undoubtedly, recent achievements in nanotechnology and the development of particles synthesis provided important tools for the fabrication of Pickering systems. The possibility to control dimensions, morphology and chemical groups on the surface made, among the others, silica particles very interesting to such aim. Hydrophilic silica spheres were used to stabilize oil-in-water emulsions by anchoring at the liquid–liquid interface and forming a protecting monolayer on the droplets external surface.<sup>[42]</sup> Mesoporous silica with tunable surface was used to successfully prepare both water-in-oil and oil-in-water Pickering emulsions.<sup>[43]</sup>

Inherently hydrophilic silica nanoparticles were modified by in situ hydrophobization with oil molecules, such as dialkyl

adipate, which enabled the formation of oil-in-water emulsions whose stability strictly depends on the chain length of the organic moiety.<sup>[44]</sup> More interestingly, it is reported that the dimensions of the final droplets can be tailored by changing the diameter of the silica particles used as solid stabilizers. Indeed, the size of the Pickering emulsions decreases with smaller silica nanospheres.<sup>[45]</sup> Also, Li et al. employed in situ polymerization of SiO<sub>2</sub> to prepare Pickering emulsions with cinnamon oil as inner core, thus possessing excellent and long-term antibacterial properties, as showed by in vivo experiments.<sup>[46]</sup>

Nonetheless, some of these “hard nanoparticles” can show side effects especially concerning health and cosmetics related applications. Therefore, the need for particles of natural origin, showing biocompatibility and environmental friendliness, has become compelling.

The particle-like nature together with the ampholytic/amphiphilic properties made proteins suitable for the adsorption at the water/oil interface of Pickering emulsions (**Figure 2**).<sup>[47]</sup>

Literature reports about the preparation of spherical emulsion droplets stabilized by  $\beta$ -lactoglobulin.<sup>[48]</sup> Plants derived proteins are preferentially used due to their higher sustainability compared to animal based products. Soy, lentils, chickpeas, and corn proteins are only a few examples.<sup>[49–51]</sup>

As a corn derived protein, zein possesses high hydrophobicity conferred by apolar aminoacids and this aspect represents an issue for the adsorption at liquid interfaces. Zou et al. reported the increase of the hydrophilic character of zein by the incorporation of tannic acid, which resulted in the formation of functional Pickering stabilizers with tunable properties.<sup>[52]</sup>

Besides, the use of polysaccharides offer many advantages since they can be easily modified to tune their main properties (e.g., hydrophobicity and charge) in order to reach the optimal conditions for the stabilization of Pickering emulsions.<sup>[53]</sup> Among them, starch granules have been widely used to prepare emulsion systems with high resistance to the variation of pH or ionic strength.<sup>[54]</sup> According to literature, this effect is most likely due to the formation of an inter-droplets network similar to a gel-like phase which confers thermo-responsive features to the system in a swelled state with barrier performances.<sup>[55]</sup> Similarly, Jiang et al. reported the preparation of Pickering emulsions gels by exploiting the gelling ability of a family of natural sulfated esters deriving from polysaccharides, namely the k-carrageenans.<sup>[56]</sup> Given the high susceptibility to K<sup>+</sup> cations and the viscoelastic and brittle properties of this class of hydrocolloids, they were employed for the fabrication of oil-in-water droplets by changing the pH, the ionic strength of the medium and the oil fraction.<sup>[56]</sup>

Due to their high aspect ratio, green and eco-sustainable cellulose nanoparticles have been widely investigated for the design of Pickering emulsions. The different types of nanocellulose showed different capability to act as solid stabilizers due to their flexibility and structural properties. Indeed, the longest and flexible BC (bacterial cellulose) has a slight effect on the formation of Pickering emulsions whereas semi-flexible CNF (cellulose nanofibers) and rigid CNC (cellulose nanocrystals) are good candidates (**Figure 3**).

In the former case the formation of droplet clusters can be observed due to the depletion effect; in the latter case, instead, the repulsive effect is dominant so that the different emulsions can be well separated.<sup>[57]</sup> Starting from this, oppositely charged cellulose nanofibrils were employed for the design of salt

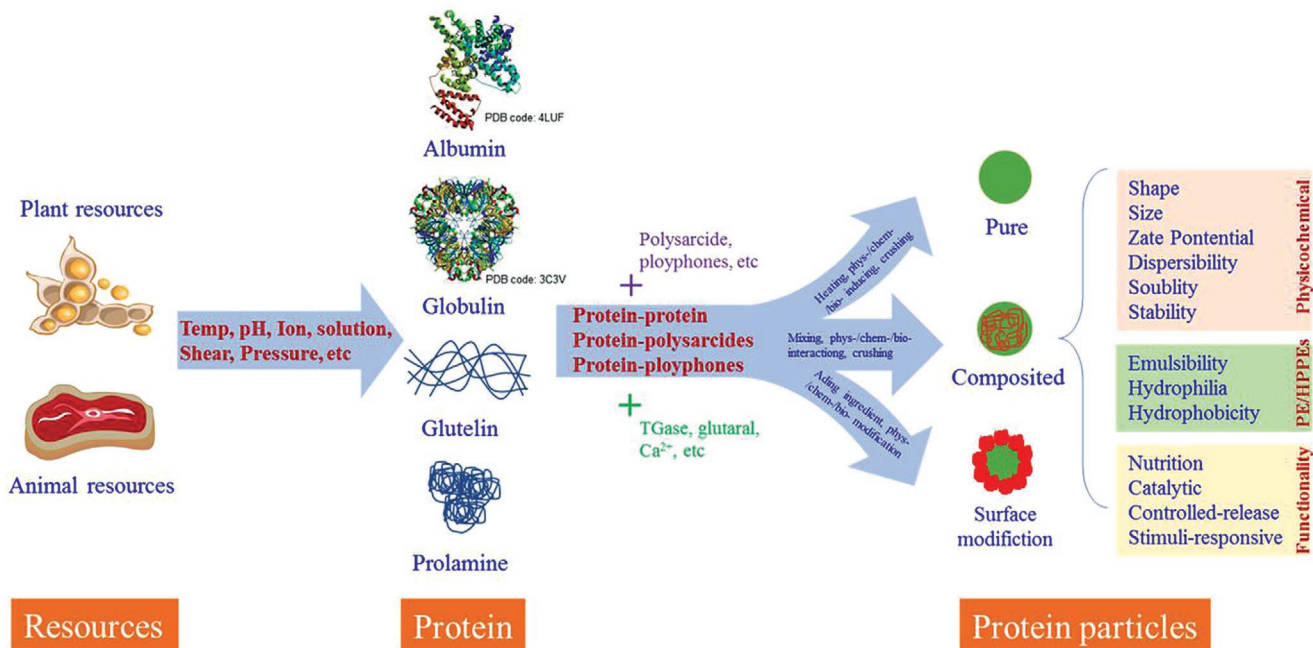


**Figure 2.** Proteins based Pickering emulsions: from the natural resource to the formation of particles. Reproduced with permission.<sup>[47]</sup> Copyright 2020, Elsevier Ltd.

responsive Pickering systems whereas cellulose nanocrystals were used for the entrapment of thymol, which is an essential oil immiscible with water, and the resulting stabilized particles showed high larvicidal activity even after being embedded into an alginate based matrix.<sup>[58,59]</sup>

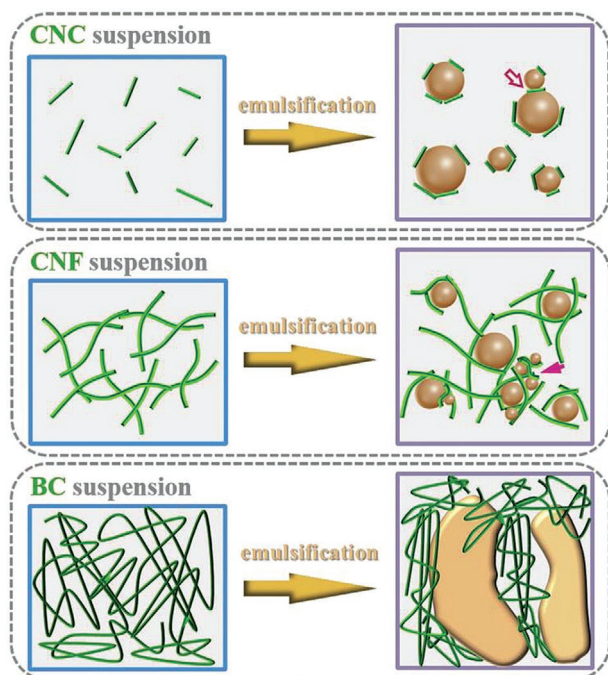


**Figure 3.** Cellulose nanocrystals (CNC), cellulose nanofibers (CNF), and bacterial cellulose (BC) as stabilizers for Pickering emulsions. Reproduced with permission.<sup>[57]</sup> Copyright 2021, Elsevier Ltd.

Moreover, in order to overcome some limitations to the use of rigid particles (e.g., difficulty to deform and petrochemical nature), also polymers based materials have been used for the design of solids stabilized emulsions systems. Among them poly(lactic acid) (PLA) and poly(caprolactone) (PCL) meet the requirement for biocompatibility, Polystyrene (PS) and poly(ethylene glycol) (PEG) were used for the fabrication of colloidosomes and for the stabilization of Pickering emulsions with a lipids based core and high coverage degree.<sup>[60,61]</sup> More interestingly, pH and temperature responsive systems were obtained by exploiting the proper features of poly(N-isopropylacrylamide-co-methacrylic acid) (PNIPAM-MAA) microgel particles, which can act a stabilizing shells by anchoring at the interface of ionic liquid-in-water droplets.<sup>[62]</sup>

In addition, carbon-based particles such as carbon nanotubes, graphene nanoplatelets or carbon quantum dots have been used for the development of Pickering emulsions to be applied in catalysis, water remediation or biosensors production.<sup>[63-65]</sup> It was also reported that food-grade products such as gelatin are necessary for the application of particle-stabilized emulsions in food industry, where safety concerns are crucial and they restrict the range of materials that can be employed for the formulation of edible products.<sup>[66]</sup>

It should be now clear that the range of particles that can be used for the design of Pickering emulsions is very broad. Then, we will try to provide more significant details about nanoclays stabilized Pickering emulsions in the following paragraph.

### 2.3. Nanoclays Based Pickering Emulsions

Clay minerals are natural occurring materials structurally composed by a tetrahedral sheet of silicon-oxygen and an octahedral

sheet of aluminum or magnesium in a six-fold coordination which are joined together by oxygen bridging to form 1:1, 2:1 and 2:1:1 phyllosilicates.<sup>[67]</sup>

A common characteristic of clay minerals is their fine grained natural structure. They can be divided into four major groups in terms of the variation in the layered arrangement: the kaolinite group, the smectite group, the illite group, and the chlorite group.<sup>[68]</sup> Nanoclays belong to this wide family and they have at least one dimension in the nanometric scale.

Due to their chemical and morphological properties, nanoclays are excellent candidates for the stabilization of Pickering emulsions. First of all, they are environmental friendly and biocompatible materials that can be used in basically all the application domains.<sup>[69]</sup> Their surface bears active groups, mainly hydroxyls, which represent anchoring sites both for molecules adsorption and for carrying out grafting reactions.<sup>[70]</sup> As a direct consequence, the wettability can be modulated to act as solid stabilizers. It was previously discussed that this is a crucial factor affecting the formation of Pickering systems.

Nanoclays can be easily dispersed in water or other organic solvents depending on their external functionalization and the viscosity of the dispersions can be controlled by volume fraction variations.<sup>[71]</sup> Most importantly, these inorganic solids display a wide spectrum of different morphologies (i.e., layered, rod-shaped, discoidal, fibrous, tubular) each of them with a proper aspect ratio, anisotropy and size range.<sup>[72]</sup>

In Equation (1) the detachment energy was firstly reported. However, it is worth to remember that Equation (1) can be only used for spherical particles. Thence, a legitimate question might arise regarding what happens for differently shaped particles.

Literature reports that the detachment energy for a disc-like particle with a negligible thickness is:<sup>[73]</sup>

$$\Delta E_{\text{det}} = \gamma_{o/w} \pi R_{\text{disc}}^2 (1 - |\cos\theta|) \quad (2)$$

where  $R_{\text{disc}}$  is the radius of the particle itself. Similarly, Peddiredy et al. deduced later that the detachment energy for a rod-like particle can be expressed as:<sup>[74]</sup>

$$\Delta E_{\text{det}} = \gamma_{o/w} lq(1 - |\cos\theta|) \quad (3)$$

where  $l$  and  $q$  are the length and width of the rod-like particle, respectively.

Insightful details about the stabilization provided by each particle can be obtained through the comparison of Equations (1), (2) and (3). Indeed, it is possible to assess that the detachment energy is a quadratic function of the term  $1 - |\cos\theta|$  for spheres and a linear function of the same term for rod- and disc-like solids. Mathematically, these observations mean that more energy is required to detach non spherical geometries from a liquid-liquid interface in Pickering emulsions compared to spherical particles, so that the former can act as stabilizers more proficiently than the latter ones.<sup>[73]</sup> One should also consider that any shape variations result in a different coverage degree, which is maximized for discs and rods since they can optimize their orientation at the interface.<sup>[75]</sup> In light of it, anisotropic particles can considerably improve the stabilization of Pickering systems due to their morphology, besides their

wettability, by irreversibly anchoring at the oil-water interface and creating a physical barrier which provides steric hindrance and inhibits Ostwald ripening and coalescence.<sup>[76]</sup> Therefore, the various nanoclay minerals with different shapes play a major role (**Figure 4**).

Literature reports the preparation of clays based emulsions by using sepiolite, palygorskite and montmorillonite. In all these cases, the interactions between the solids and the liquid phases provided a strong barrier and limited the movements of the droplets, thus avoiding their coalescence according to the rheological properties of the systems. The presence of nanoclays in the continuous phase is responsible for the increase of the viscosity, which also represents a stabilizing factor.<sup>[77]</sup>

Moreover, the type and concentration of nanoclays affects the size of the final droplets which decreases when the particles amount becomes higher as reported for, among others, montmorillonite and nonionic surfactants co-stabilized emulsions.<sup>[78]</sup> Also, Lu et al. investigated that the dimensions of attapulgite nanorods stabilized droplets increased with increasing pH values as a proof of the tunable interactions arising between the clay and pH responsive chitosan.<sup>[79]</sup>

Laponite, which is a synthetic layered magnesium silicate from the hectorite group, was also employed as stabilizer given its reversible thixotropic behavior and high negative net charge.<sup>[80]</sup> Stable emulsions were prepared by increasing the ionic strength of toluene-in-water mixtures due to the screening of repulsive forces. Otherwise, an increase of the clay concentration rather than the ionic strength can also provide stability if it is high enough to induce the gel-like phase, which is capable to overcome the repulsions.<sup>[81]</sup> Among the different applications, Yu et al. reported the use of laponite as stabilizer for alkenylsuccinic anhydride (ASA) droplets, after being modified with carbon nitride quantum dots to become partially hydrophobic, for sizing procedures in the paper-making industry.<sup>[82]</sup>

Similarly, montmorillonite particles can be modified with surfactants to minimize the negative charge thus leading to organophilic nanoclays that show high stabilizing efficiency for the oil phase in a multiple emulsion system.<sup>[83]</sup> To give an example, silane functionalization of montmorillonite platelets increased the stability of oil-in-water emulsions and provided a nucleation site for the formation of latex particles. Hence, clay hydrophobic polymer latex nanocomposites with a clustered structure were fabricated by using styrene and n-butyl acrylate.<sup>[83]</sup>

Kaolinite, which is the most representative clay in the group which takes its name, has also been extensively investigated for the preparation of Pickering emulsions. In particular, it was reported that nanosheets display the ability to orient at the interface and to form oil-in-water emulsions in the presence of nut oil.<sup>[84]</sup> If the phase fraction increases, kaolinite particles migrate from the water to the oil phase and form oil-in-water droplets, due to the interactions between the clay surface and the free fatty acids in the oil.<sup>[84]</sup> Similarly to the other clays, the surface of kaolinite can be modified by the addition of surfactants in order to tailor its wettability. Neat nanosheets cannot stabilize paraffin and formamide droplets because of the lack of electrostatic effects whereas, after the modification with non-ionic species, three months long stable emulsions can be

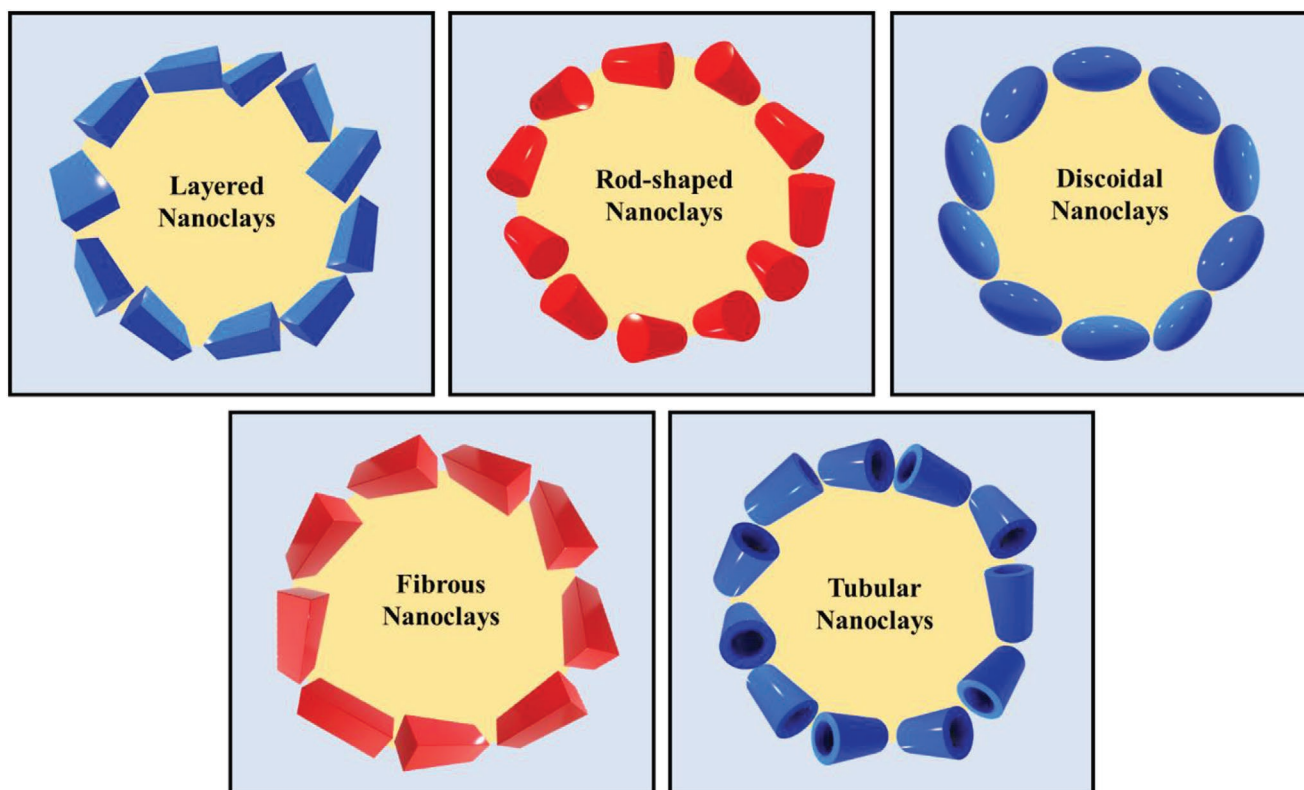


**Figure 4.** Nanoclays with different morphologies for the stabilization of Pickering Emulsions.

fabricated.<sup>[85]</sup> Here again, pH and ionic strength, concentration and volume fractions play a major role together with wettability. It is worth to note that the chemical nature of kaolinite is the same as halloysite nanotubes, which will be the main focus of the following paragraphs.

### 3. Halloysite Nanotubes Based Pickering Emulsions

#### 3.1. A Hollow Nanotubular Clay with Peculiar Features

Halloysite nanotubes (HNTs) are natural occurring 1:1 phyllosilicates with unit formula identical to kaolinite, namely  $\text{Al}_2\text{Si}_2\text{O}_5(\text{OH})_4 \cdot n\text{H}_2\text{O}$ , and they belong to the same clay group.<sup>[86]</sup> HNTs are composed by the alternation of a tetrahedral sheet of Si-O-Si overlapping an octahedral sheet of Al-OH and the resulting layered kaolinite-like structure furtherly rolls up, thus conferring the clay its very peculiar hollow nanotubular morphology (Figure 5).<sup>[87–89]</sup> The difference between HNTs and kaolinite structural organization is most likely related to some packing disorder caused by the presence of two water molecules in the interlayer volume.<sup>[90]</sup> Indeed, the  $n$  coefficient in the chemical formula of halloysite indicates the number of  $\text{H}_2\text{O}$  units, and it can be 0 or 2. Depending on it, halloysite can be classified as anhydrous or hydrated and the distance between each of the 15–20 rolling layers can be 0.7 or 1 nm, respectively.<sup>[91]</sup> The dimensions of the nanotubes depend on their natural source of extraction and they can be polydisperse. The

external diameter is in the range of 50–200 nm, the internal diameter can be from 15 to 50 nm and the tubes length is 1–2  $\mu\text{m}$ .<sup>[92,93]</sup>

The different chemistry between the external (composed of Si based tetrahedrons) and the internal (composed of Al based octahedrons) surfaces provides halloysite with its most interesting property. Indeed, the former is negatively charged and the latter is positively charged in a wide pH range, from 2 to 8.<sup>[94,95]</sup> As a consequence, it is possible to selectively functionalize the different surfaces of halloysite by exploiting electrostatic interactions with ionic molecules and charged species.<sup>[94,96]</sup> Cavallaro et al. demonstrated that anionic surfactants (e.g., sodium alkanoates) can be adsorbed into the inner lumen of HNTs and the final net negative charge of the nanotubes increases, thus providing a higher contribution of the electrostatic repulsions and enhanced dispersion stability.<sup>[97]</sup> According to the DLVO theory, the stability of a colloidal system is related to the balance between the attractive van der Waals forces and electrostatic repulsions caused by the double layer surrounding each particle but, at the same time, the ionic strength also plays a role in screening the repulsive forces due to the reduction of the double layer width.<sup>[98]</sup> The result of the selective functionalization with anionic species inside the inner positive lumen of halloysite is the creation of inorganic micelles, with a hydrophilic shell and a hydrophobic core, which can be used for the efficient removal of pollutants and hydrocarbons (both aliphatic and aromatic).<sup>[99]</sup> Contrarily to it, instead, inorganic reverse micelles in non-aqueous media can be easily prepared by the functionalization of HNTs outer

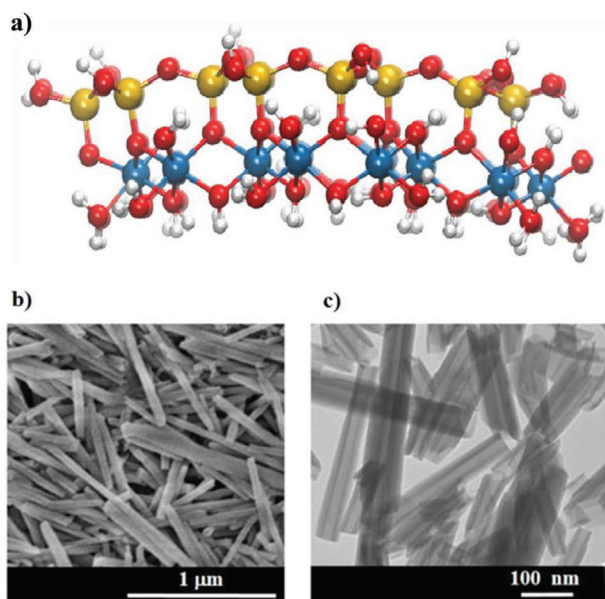


**Figure 5.** a) Halloysite model surface: H atoms are in white, O in red, Si in yellow, and Al in blue. Reproduced with permission.<sup>[87]</sup> Copyright 2017, American Chemical Society. b) SEM and c) TEM images for halloysite clay nanotubes. Reproduced with permission.<sup>[89]</sup> Copyright 2020, American Chemical Society.

negative surface with cationic surfactants, such as alkyltrimethylammonium bromides.<sup>[100]</sup> In this case, the system displays a hydrophilic core and a hydrophobic shell that generate an aqueous nano-pool in organic media. This particular class of reverse micelles possesses different dispersibility in organic solvents and they can be exploited for the stimuli responsive release of active cargos.<sup>[101,102]</sup>

Halloysite nanotubes have been widely investigated in the recent times and they have been exploited for a broad range of applications due to their peculiar morphology and high aspect ratio, the different chemistry and opposite charges at the internal/external surfaces, the presence of a nanoscaled lumen suitable for either the loading or the delivery of molecules, the affordable low cost and for their biocompatibility and no-toxicity shown in several *in vitro* and *in vivo* assays.<sup>[103–109]</sup> Literature reports many studies dealing with the encapsulation of biologically and chemically active compounds within the inner lumen of HNTs, each of them taking into account the electrostatic interactions between the molecules and the nanoclay as driving force.<sup>[110–114]</sup> The most crucial step in the whole procedure for the loading of nanotubes consists in a vacuum pumping in/out operation, where the host/guest dispersion is brought from atmospheric pressure to a vacuum jar in order to optimize the amount of encapsulated species by keeping the system under low pressure conditions for 1–5 h and then cycling it back to atmospheric values. Generally, this operation is repeated for 3 times. Price et al. firstly reported the loading of Tetracycline, Khellin, and Nicotinamide Adenine Dinucleotide into halloysite by vacuum pumping and they observed an overall slight fizzing of the HNTs suspension inside the jar.<sup>[115]</sup> At the beginning, this phenomenon was related to the removal of air from the inner volume of nanotubes with the consequent

enhancement of filling efficiency.<sup>[116]</sup> However, it was recently found that the slight fizzing can be explained by the removal of water from a confined space due to its larger vapor pressure and, consequently, faster evaporation rate that can be attributed to the Gibbs-Thomson effect, both in aqueous and organic media.<sup>[117,118]</sup>

Starting from these observation, different drug delivery systems were developed. For instance, non-steroidal anti-inflammatory drugs (NSAIDs) and antibiotics were encapsulated within the lumen of HNTs and a broad range of different functional smart nanomaterials for health applications were prepared in combination with polymers, biopolymers or surfactants.<sup>[119–121]</sup> The development of halloysite/keratin nanocomposites for the photoprotection of human air was also reported.<sup>[89]</sup> Besides, the preparation of poly ( $\epsilon$ -caprolactone) (PCL) based nanocomposites with embedded lysozyme loaded halloysite was carried out to design antimicrobial membranes for food packaging applications.<sup>[122]</sup> Similarly, antioxidant species were loaded inside the nanoclays for the protection and long-term storage of food.<sup>[123]</sup> The creation of self-healing protective coatings was also reached by loading HNTs cavity with corrosion inhibitors (e.g., benzotriazole) that can be added to paints for the improvement of both the anticorrosion performances and the coating tensile strength.<sup>[124–126]</sup> Moreover, halloysite has been widely investigated for catalytic purposes as well as for oils and chemicals capture in environmental remediation, for the treatment and conservation of cultural heritage, the development of cementitious materials for building technology and as nanofillers for the design of novel bioplastics with enhanced thermo-mechanical properties.<sup>[127–136]</sup>

### 3.2. HNTs as Interfacially Active Stabilizers

As a consequence of their numerous advantages (low cost, biocompatibility, environmental friendliness, mechanical strength, different surface charges, hollow tubular morphology, etc.) and their switchable partial surface wetting properties, Halloysite Nanotubes are efficient candidates as interfacially active inorganic particles for the formation of Pickering emulsions.

Assuming the geometry of a solid cylinder with flat faces and with a three-phase contact angle, as shown in **Figure 6a**, it is possible to approximate the tubular morphology of HNTs.<sup>[137]</sup> According to what was previously discussed in the general overview, the emulsion system can be destabilized by particles desorption to the bulk phases and the contact angle at the oil-water interface is the parameter defining which phase will be preferred. Since halloysite-water-oil three phase contact angle is  $<30^\circ$  ( $25.6 \pm 0.1^\circ$  for halloysite – water – dodecane interface measured by the compressed tablet method), pristine clay particles will more proficiently stabilize emulsions having H<sub>2</sub>O as bulk phase.<sup>[138]</sup>

HNTs desorption from the oil-water interface to the aqueous bulk phase can be considered as the most thermodynamically favorable scenario. As a consequence, the study of the surface free energy for cylindrically shaped particles results in a detachment energy ( $\Delta E$ ) from the interface to water that can be expressed as reported by Owoseni et al.:<sup>[137]</sup>

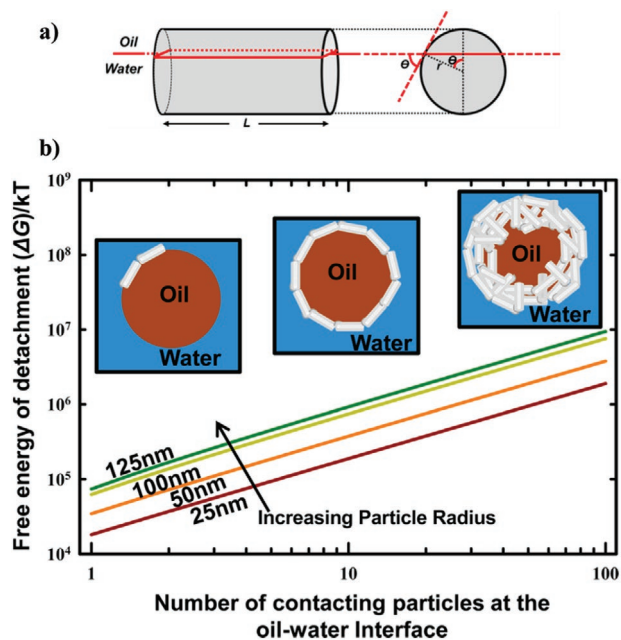


**Figure 6.** a) Cylindrical geometry of halloysite in a side-on orientation at a planar oil–water interface. b) Variation of free energy of detachment with number of contacting cylindrical particles in capillary aggregates trapped at the oil–water interface. Cylinders possess a length of 1  $\mu\text{m}$  with radius ranging from 25 to 125 nm. Reproduced with permission.<sup>[137]</sup> Copyright 2014, American Chemical Society.

$$\Delta E_{\text{det}} = 2rL\gamma_{\text{o/w}} \left( \sin\theta - \theta\cos\theta - \frac{r\theta\cos\theta}{L} + \frac{r\cos^2\theta\sin\theta}{L} \right) \quad (4)$$

where  $\theta$  is the three phase contact angle,  $\gamma_{\text{o/w}}$  is the interfacial tension between oil and water,  $L$  and  $r$  are the length and radius of the cylinder, respectively.

By taking into account the dimensions of halloysite,  $\approx 1 \mu\text{m}$  long cylinder with radius  $\approx 50 \text{ nm}$ , the three phase contact angle which is  $25.6^\circ$  when dodecane is the oil phase, and the dodecane–water interfacial tension of  $49 \pm 1 \text{ mN m}^{-1}$  then it is possible to calculate the detachment energy. For this system  $\Delta E_{\text{det}}$  is  $(3.45 \times 10^4)kT$ , meaning that the particles are irreversibly adsorbed at the interface.<sup>[139]</sup>

Literature also reports that the existence of capillary interactions between small particles due to the formation of a meniscus at the oil–water interface.<sup>[140]</sup> These attractive forces, which typically overcome the thermal energy ( $kT$  factor), can strongly affect the network of particles at the fluid interface, thus provoking their interconnection and the formation of aggregates.<sup>[141,142]</sup>

For that concerns Halloysite Nanotubes, they are jammed together at the interface in a chain-like assembly of cylindrical particles whose final length is greater than the proper length of a single nanotube,  $L' > L \gg r$ . Hence, Equation (4) can be rewritten as:<sup>[137]</sup>

$$\Delta E_{\text{det}} = 2rL'\gamma_{\text{o/w}} (\sin\theta - \theta\cos\theta) \quad (5)$$

As shown in Figure 6b, the energy of detachment increases with the particle radius and, most interestingly, with the

number of particles interconnecting by end-to-end linkages. Indeed, the energy needed for the desorption of a network of 10 nanotubes, all of them approximately possessing a radius of 50 nm and a length of 1  $\mu\text{m}$ , increases by one order of magnitude compared to the desorption of a single nanotube. This enhancement of the energy of attachment is the result of capillary interactions, which provide a strong contribution and play a major role in halloysite anchoring at the oil–water interfaces.<sup>[137]</sup>

Similar observations were made by Kpogbemabou et al., who investigated the preparation of oil-in-water Pickering emulsions stabilized with three different pristine clays at high concentration: namely 15 wt% of either halloysite or kaolinite or attapulgite in the water phase. Notwithstanding the same chemistry, halloysite can stabilize the system at higher oil fractions compared to kaolinite. This effect is most likely related to the higher specific area (i.e.,  $28 \text{ m}^2 \text{ g}^{-1}$  for halloysite and  $11 \text{ m}^2 \text{ g}^{-1}$  for kaolinite, respectively), as a consequence of the different morphological features.<sup>[143]</sup>

The prepared emulsions displayed similar long-term stability even if no surface treatment was carried out for the three clays and only a limited coalescence could be observed. Also, similar values of droplet size and droplet size distribution were found, regardless of the specific clay. More interestingly, rheological studies enlightened the different behaviors between halloysite, kaolinite and attapulgite.<sup>[143]</sup> For instance, halloysite based systems exhibited the highest yield stress and elastic modulus, which is two order of magnitude larger than those of kaolinite and palygorskite. Also, halloysite-based emulsions possess the highest cohesive energy compared to kaolinite- and palygorskite-based emulsions which, instead, show similar behaviors. The three systems have a gel-like structure. The most rigid structure, the highest cohesive energy and the lowest critical deformation of halloysite based emulsions clearly indicate that a strong network of nanotubes formed at the oil–water interface due to the strong interactions between the elongated cylindrical particles, thus enhancing their stability and cohesion.<sup>[143]</sup>

Similarly, Cai et al. investigated the formation of Pickering emulsion by using HNTs with uniform morphology prepared from kaolinite.<sup>[144]</sup> The stability was studied through the evaluation of the emulsion volume fractions and the calculation of the Creaming Index (CI), defined as:

$$\text{CI} = \left( \frac{h_e}{h_t} \right) \times 100\% \quad (6)$$

where  $h_e$  is the volume of the emulsion layer and  $h_t$  is the total volume of the sample after stratification and separation. Hence, a higher Creaming Index indicates a higher stability.

After a 3 weeks long equilibration period, the CI was 76% for HNTs based emulsions and 56% for the kaolinite based emulsions, respectively. Thus, halloysite could act as a better emulsifier than its sheet-like precursor. Similar behaviors were found even after centrifugation.<sup>[144]</sup> The reason of halloysite better performance has to be found in its ability to form a regular and ordered single layer of closely packed nanotubes at the water–oil interface thank to their uniform shape and size, thus hindering the coalescence of droplets and their aggregation. On the other side, clay sheets cannot assembly in a well-organized structure at the interface. Here again, viscosity plays a major



role. It is reported that the viscosity of HNTs based systems is 2.5 times that of kaolinite based counterparts, accounting for better stability.<sup>[144]</sup>

We have already reported that the formation and stabilization of Pickering emulsions is strongly dependent on the wetting properties of the particles.<sup>[145]</sup> Hydrophilic particles can stabilize oil-in-water emulsions whereas hydrophobic particles can stabilize water-in-oil emulsions. It is also worth to note that strongly hydrophilic/hydrophobic particles could not act as droplets stabilizers but they could remain in the aqueous/oil phase, instead. For what concerns halloysite nanotubes, the presence of Si-OH groups on the external surface is crucial for the modification of the clay, whose wettability can be tuned from hydrophilic to hydrophobic. Undoubtedly, this factor will affect the type and the main characteristics of the resulting Pickering emulsions.

Literature reports the use of  $\gamma$ -Aminopropyltriethoxysilane ( $\gamma$ -APTES) for such purpose. Sadeh et al. investigated the adsorption of HNTs and APTES modified HNTs at the water-palm oil interface to provide meaningful details.<sup>[146]</sup> In particular, they found that the adsorption coverage density at the interface increases with the concentration of halloysite until a critical micellar concentration (CMC) is reached. In this condition, the coverage density reaches its maximum value and it remains stable upon further addition of clay.

Moreover, the study of the interfacial tension as a function of time showed that its decrease is higher for APTES-HNTs compared to pristine HNTs and the interfacial tension reaches a quasi-equilibrium state when the interface is completely covered by a monolayer of nanotubes. In both cases, the prepared emulsions were stable over a period of 4 weeks and neither creaming nor sedimentation were observed. Wettability studies showed that APTES-HNTs were hydrophobic and pristine HNTs were hydrophilic, given the values of their contact angles ( $97 \pm 2^\circ$  and  $29 \pm 1^\circ$ , respectively). As a direct consequence, the former resulted in W/O emulsions and the latter in O/W emulsions, as experimentally demonstrated.<sup>[146]</sup>

Ouadaker et al. exploited the formation of halloysite stabilized Pickering emulsions as templates for the design of porous granules via freeze granulation.<sup>[147]</sup> For this purpose, the emulsion was atomized and frozen by spraying it into liquid nitrogen. Then, a freeze-drying step under vacuum conditions allowed for the sublimation of ice thus leading to the formation of macroporous capsules which could retain the initial morphological features. In order to get a better control of the formulation, the effect of pH and ionic strength was investigated together with the addition of organic binders (poly(vinyl alcohol) (PVA) and poly(ethylene glycol) (PEG)). It was observed that the increase of pH from 3.4 to 7 is responsible for a rapid creaming of the system. This effect is most likely due to the charge transition from positive to negative on the inner surface of halloysite, with an overall shift of its  $\zeta$ -potential toward more negative values. Hence, the extent of repulsive interactions between HNTs and the oil increases and the emulsion breaks. Contrarily to that, it was also reported that the concentration of NaCl does not influence the stability of the Pickering system and its  $\zeta$ -potential: all emulsions were stable during several weeks, regardless the significant variation of conductivity (from  $0.1 \text{ mS cm}^{-1}$  without NaCl to  $9 \text{ mS cm}^{-1}$  for  $[\text{NaCl}] = 0.1 \text{ M}$ ).

These findings could be explained by invoking the adsorption of  $\text{Na}^+$  and  $\text{Cl}^-$  ions on the surfaces of halloysite.<sup>[148]</sup> To conclude, electrostatic interactions play a major role on the main features of the emulsions. A highly negative surface is not recommended for stabilization, which is reached with medium zeta potential values.<sup>[147]</sup> Furthermore, the addition of different concentration of PVA and PEG also affected the preparation of both Pickering emulsions. After their adsorption on halloysite surface via hydrogen bonding, these polymers provided a steric contribution and increased the hydrophobicity of the clay. **Figure 7a** shows SEM images of the porous granules after freeze-drying of Pickering emulsions at pH = 3.4 with different concentrations of binders.

It is clear that all granules have spherical shape and their size distribution increases with the concentration of PVA and PEG

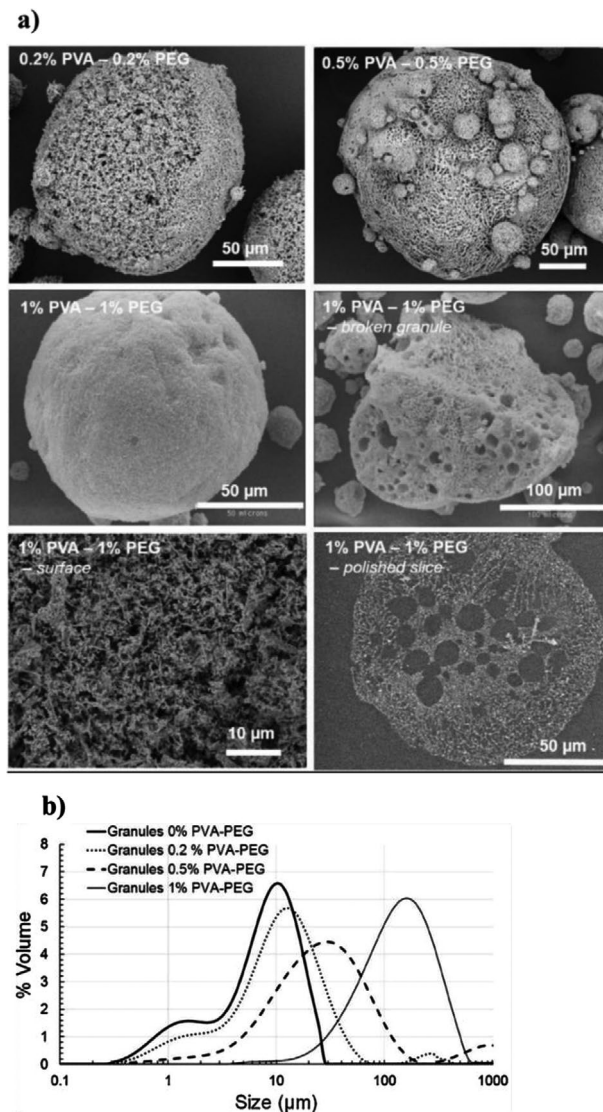


**Figure 7.** a) SEM images of powders obtained by freeze granulation from halloysite emulsions with different concentrations of PVA and PEG. b) Dimensions of granules obtained by freeze granulation of halloysite emulsions at natural pH with 0 – 0.2% – 0.5% – 1% PVA and PEG. Reproduced with permission.<sup>[147]</sup> Copyright 2020, Elsevier Ltd.

(Figure 7b). Many pores could be observed when the content of organic polymers is low but, on the other side, the surface became smoother and more homogeneous when the concentration increased up to 1%. Halloysite nanotubes could be observed on the outer surface and porosities still exist, as shown by SEM images of the polished cross section. The binders are needed to retain the structure and give enough cohesion.<sup>[147]</sup> Moreover, these materials may have a high potential for the encapsulation of organic substances or as support for catalytic purposes. Similarly, Buruga et al. synthesized Poly(styrene-co-methylmethacrylate) (PS-co-PMMA) nanospheres by the ultrasound-mediated polymerization of halloysite stabilized Pickering nanoemulsions. The resulting material can find applications in medicine, dentistry, paper, paint, and automotive industries.<sup>[149]</sup>

In their recent work, Stehl et al. reported the preparation of halloysite stabilized dodecene-in-water Pickering emulsions that can be used for all those applications requiring an efficient filterability.<sup>[150]</sup> To give an example, the final step of an homogeneously catalyzed reaction is the separation of the catalyst from the products as part of a recyclable process. In this context, one could carry out the reaction either in a system composed by two immiscible phases or, as an alternative, in a system composed by two completely miscible phases. However, both cases present an issue: small contact area between the reactants (which

means low conversion rate) for the former case or difficult separation procedure for the latter case. The use of Pickering emulsions can overcome these disadvantages and it can provide both high contact area and simple filterability (Figure 8).

As a matter of fact, the attachment of nanotubes at the oil/water interface is irreversible being the calculated  $\Delta E_{\text{det}} = 22\,582\text{ kT}$  ( $T = 295.15\text{ K}$ ), which is 4 orders of magnitude higher than the thermal energy  $kT$ . HNTs are laterally oriented and bundled together.<sup>[150]</sup>

In this study, the concentration of the clay was increased from 0 to 1 wt% and it was observed that the emulsions are successfully stabilized against coalescence and phase separation. More interestingly, the increase in concentration leads to a nonmonotonous decrease of droplets size which can be attributed to some changes in the packing parameter and to the coverage of the emulsions. In particular, halloysite nanotubes are isotropically oriented at low concentration and they re-organize in a radial side-to-side configuration at high concentration.

Finally, the membrane filtration experiments showed that the emulsions could be concentrated up to over 90 vol% oil phase and still be easily separated as suggested by the formation of a halloysite layer on top of the membrane.<sup>[150]</sup>

These results demonstrated the high potential to use halloysite based Pickering emulsion in many technological applications such

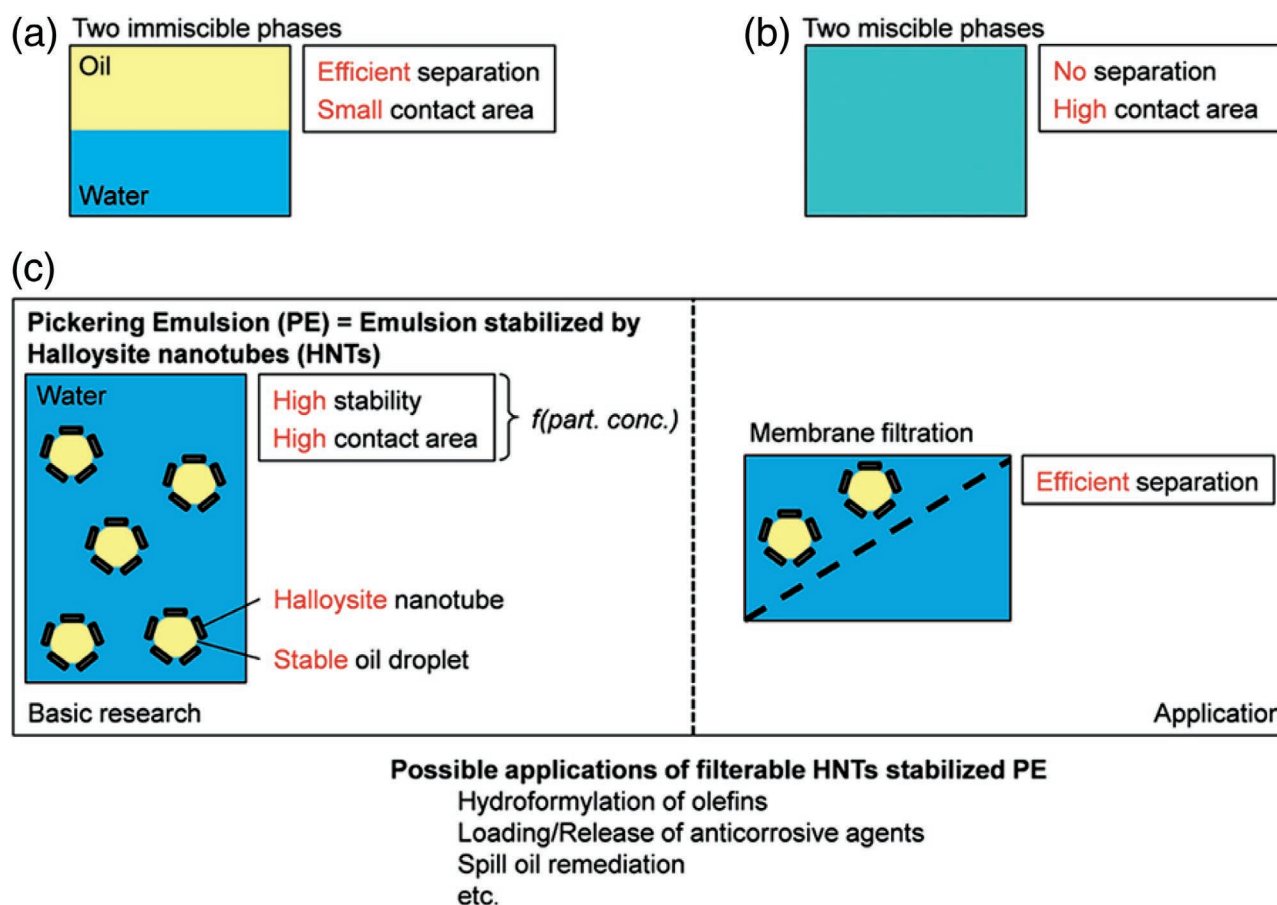


**Figure 8.** Schematic Illustration of Three Different Systems: a) A system composed of two immiscible phases, b) a system composed of two completely miscible phases, and c) the application of Pickering emulsions stabilized by halloysite nanotubes for membrane filtration. Reproduced with permission.<sup>[150]</sup> Copyright 2020, American Chemical Society.

as catalysis, loading/release of active species, oil spill remediation, etc. These aspects will be discussed in the next paragraphs.

## 4. Applications of Halloysite Stabilized Pickering Emulsions

### 4.1. HNTs Based Pickering Emulsions for Environmental Purposes

Ecological sustainability has become a major societal concern and environmental protection has represented a compelling challenge in the last decades.<sup>[151]</sup> Unfortunately, the global population had to deal with large scale disasters quite often. In 2010 an explosion on the Deepwater Horizon (DWH) oil well drilling platform started one the largest oil spill in the world's history. In that occasion, several millions of crude petroleum barrels were released in the Gulf of Mexico.<sup>[152]</sup> It is well known that oil spill can detrimentally affect the health of plants and animals both in the marine and in the coastal environments. Also, human health can experience several problems because of it.<sup>[153]</sup> As a consequence, many efforts were made to develop oil spill remediation technologies.

The addition of dispersants, which are mainly surfactants, for the emulsification of the spills represents one of the most efficient procedures. For instance, it is reported that over 2.1 million gallons of Corexit EC 9500A, which is made of anionic and nonionic surfactants, were employed during the DWH disaster.<sup>[154]</sup> The reason has to be found in the capability of surfactants to reduce the oil-water interfacial tensions and to break the oil into tiny droplets which can be degraded by the action of naturally occurring degrading microorganisms, including *Alcanivorax borkumensis* and *Cycloclasticus pugetti*.<sup>[154,155]</sup> Also, "marine oil snow" flakes consisting of bacteria, dispersed oil and suspended microparticles can form and precipitate at the bottom of sea, being denser than water.<sup>[156]</sup> To do it, the surfactants must be dissolved in organic solvents (i.e., propylene glycol and petroleum distillates) but the employ of large amounts of surfactants and hydrocarbon solvents caused additional concerns about their impact on the ecosystem and the disposable income.<sup>[157]</sup> Hence, it is important to develop environmental-friendly technologies for the treatment of oil spills by minimizing the use of toxic species.

Owoseni et al. reported the use of halloysite for oil spill remediation by exploiting the capability of the clay to act as stabilizer in Pickering emulsions. More interestingly, the inner volume of nanotubes was loaded with COREXIT 9500 representative surfactants which can be furtherly released. Surfactants and halloysite nanotubes can act synergistically to stabilize the emulsion: the adsorption of surfactant molecules at the interface can decrease the interfacial tension of oil/water interface while the attachment of HNTs provides a steric barrier to drop coalescence.<sup>[137]</sup> Dodecane-in-water optical micrographs are reported in **Figure 9** and it can be clearly observed that Pickering emulsions formed even without any surfactants addition and they are stable for more than 3 months. Also, it is worth to note that the diameter of the droplets is smaller as the concentration of HNTs increases. Cryo-SEM imaging showed that each oil droplets is covered by a layer of interconnected nanotubes assembled in a side-on orientation, being this network

denser at higher clay concentration. Hence, the formation of a rigid and protective interfacial shell which provides rigidity and steric hindrance to coalescence was confirmed.<sup>[158]</sup>

The synergistic effects of halloysite and surfactants were investigated through the encapsulation of DOSS, TWEEN 80 and SPAN 80 in multiple combinations and applied to crude oil droplets without the use of any hydrocarbon solvents.

Herein, it was found that the release of the organic species from the clay lowers the crude oil-in-saline water interfacial tension, which is effectively reduced to the appropriate level for oil spill remediation.<sup>[159]</sup> In this case, the size of emulsions is smaller than those prepared with pristine halloysite as unique emulsifier and these smaller droplets will expose a larger area to the final degradation operated by marine indigenous bacteria.<sup>[137]</sup>

In order to prevent the instantaneous release of surfactants from the inner lumen of halloysite, literature also reports about the use of end stoppers which can control the delivery.<sup>[160]</sup> For instance, the preparation of a 2D metal-organic framework formed by coordinating Fe(III) with phenolic compounds, then called metal-phenolic networks (MPNs) was exploited to coat the nanotubes and to keep the surfactants inside them. In this case, a synergistic effect between the attachment of the clay at the outer surface of oil droplets and the subsequent release of the organic molecules plays a role in stabilizing the Pickering emulsions as well. The combination of the steric contribution with the decrease of the interfacial tension is efficient for spill remediation. In particular, the MPN can be formed after the loading of Tween 80 within the nanotubes and it can be furtherly dissolved at acidic pH values, typical of marine environments, through protonation of hydroxyl groups which breaks the metal coordination. According to literature the MPN coating represents 12% in weight without changing the morphology of halloysite except for a slight variation in thickness. Indeed, the external diameter of nanotubes increased from  $62 \pm 2$  nm in pristine HNTs to  $85 \pm 13$  nm in the MPN-Tween80-HNTs.<sup>[160]</sup> As it was discussed for Equations (4) and (5), the three-phase contact angle is a crucial parameter for the stabilization of emulsions. Here, the coating of halloysite resulted in an increase of this value from  $32 \pm 3^\circ$  for pristine HNTs up to  $78 \pm 3^\circ$  for MPN-Tween80-HNTs, thus approaching  $90^\circ$ , which is the optimal value for stabilizing Pickering emulsions. The calculation of the  $\Delta E_{\text{det}}/kT$  led to  $1.52 \times 10^8$  meaning that the nanotubes are strongly attached with a side-on alignment at the external surface of droplets, which are  $182.9 \pm 14 \mu\text{m}$  in size and stable for 2 weeks. Then, the pH-responsive release of surfactants can reduce the interfacial tension to allow the droplets to be suspended in the water column and separated. It should be noted that the use of end stoppers is needed to avoid any organic solvents based formulations and just water can be used in the whole procedure.<sup>[160]</sup>

Farinmade et al. also designed an innovative approach to seal surfactants inside the lumen of halloysite to avoid their immediate release.<sup>[161]</sup> In particular, HNTs can be coated by a thin layer of wax, which then dissolves upon contact with the oil droplets. **Figure 10** reports the preparation scheme.

Firstly, halloysite can be loaded with the nonionic Tween 80 surfactant, used as model being an intrinsic component of COREXIT 9500EC. This step was conducted by carrying out

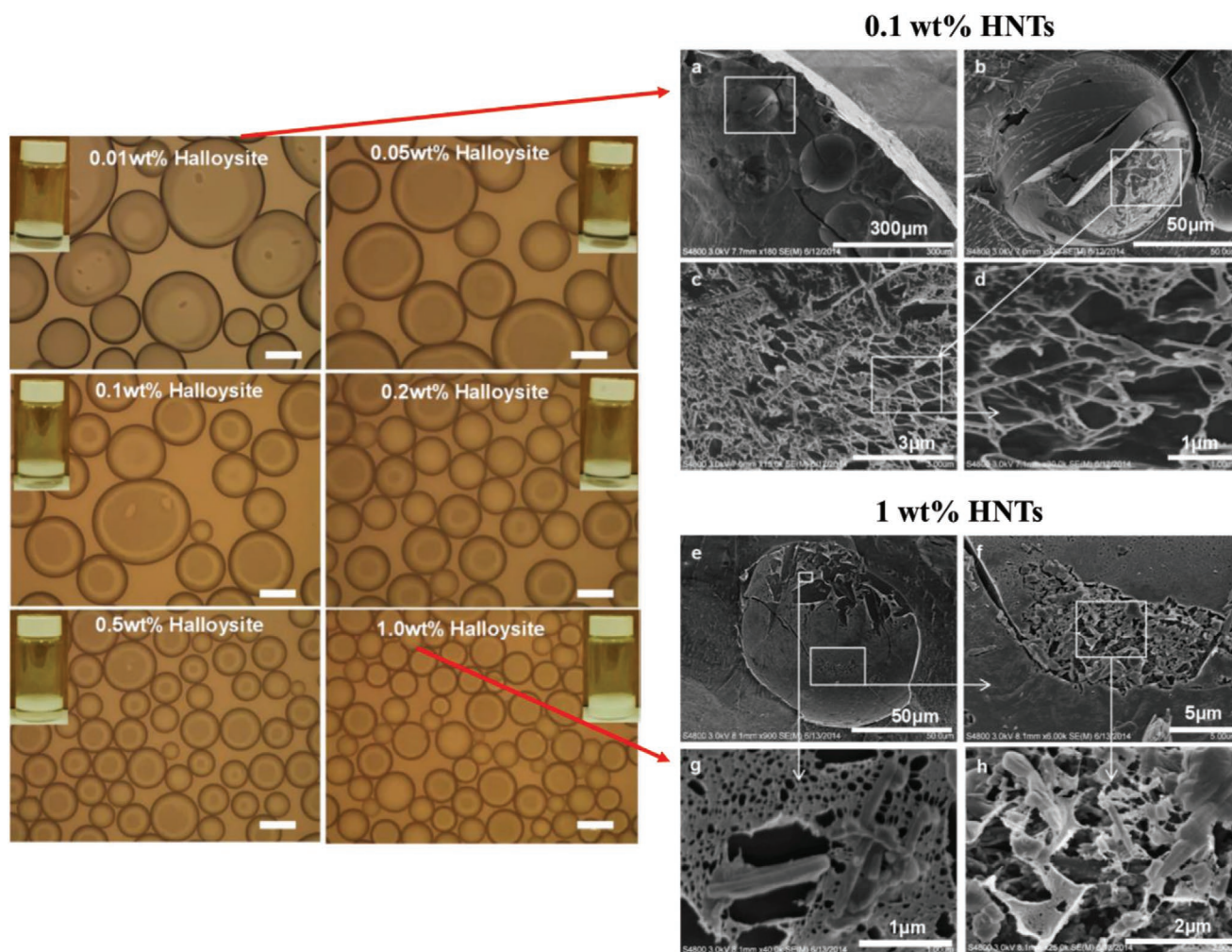


**Figure 9.** Optical microscopy images of dodecane-in-water emulsions with different concentration of HNTs. Scale bars = 100  $\mu\text{m}$  (left). Cryo-SEM images of dodecane-in-water emulsions stabilized by HNTs. HNTs concentrations are 0.1 wt% (a–d) and 1 wt% (e–h). Reproduced with permission.<sup>[137]</sup> Copyright 2014, American Chemical Society.

vacuum pumping cycles to optimize the encapsulation efficiency. Then, the wax coating of surfactant-loaded halloysite nanotubes (S-HNTs) was achieved by dip-coating them in molten paraffin and air drying to allow the wax layer to solidify and form the wax-coated surfactant-loaded HNTs (WS-HNTs).

Here again, authors reported that the nanotubes morphology is preserved after coating, with an increase in diameter from 60–80 nm for the pristine clay to 120–180 nm for WS-HNTs. The three-phase contact angle changed as well, from  $8^\circ$  for HNTs up to  $54^\circ$  WS-HNTs, accounting for higher hydrophobicity. Also, electrostatic repulsions became less strong, being the  $\zeta$ -potential  $-2.5 \pm 2$  mV after coating, whereas it was  $-20 \pm 3$  mV for bare halloysite. Release studies showed that the wax shell can effectively control the delivery of surfactants, which is delayed compared to S-HNTs.<sup>[161]</sup>

Interfacial tension measurements showed that W-HNTs had no effects, whereas the WS-HNTs systems caused a fall of the oil-water interfacial tension to values below  $15 \text{ mN m}^{-1}$  within 2 min, as a consequence of wax dissolution and surfactants release after the interaction with the oil. The formed Pickering

emulsions are stable for a month and they have a diameter of  $13 \pm 8 \mu\text{m}$ , below the  $50 \mu\text{m}$  threshold for stable drops that can be dispersed in the water column.<sup>[162]</sup> Hence, the stabilization of droplets by stimuli responsive WS-HNTs, which trigger the release of the organic payload after contact with the oil phase, represents an efficient strategy for oil spill remediation and it avoids the use of organic solvents. Being wax also a hydrocarbon, it can be easily degraded by marine organisms such as *Alcanivorax borkumensis*.<sup>[163]</sup>

Yu et al. reported the functionalization of halloysite with amphiphilic polypeptoid polymers by surface-initiated ring-opening polymerization method to be exploited as solid stabilizers for oil spill remediation.<sup>[164]</sup> Most interestingly, they found that the hydrophilicity and lipophilicity balance (HLB) deeply affects the stabilizing efficiency of the modified clay. The HLB factor is defined as the mass fraction of the hydrophilic segments over the entire mass of the whole grafted polymer and it can be adjusted by controlling the initial ratio of hydrophobic and hydrophilic monomers. Also, HLB displays higher values the more hydrophilic the polypeptoid is.<sup>[165]</sup> In order to evaluate

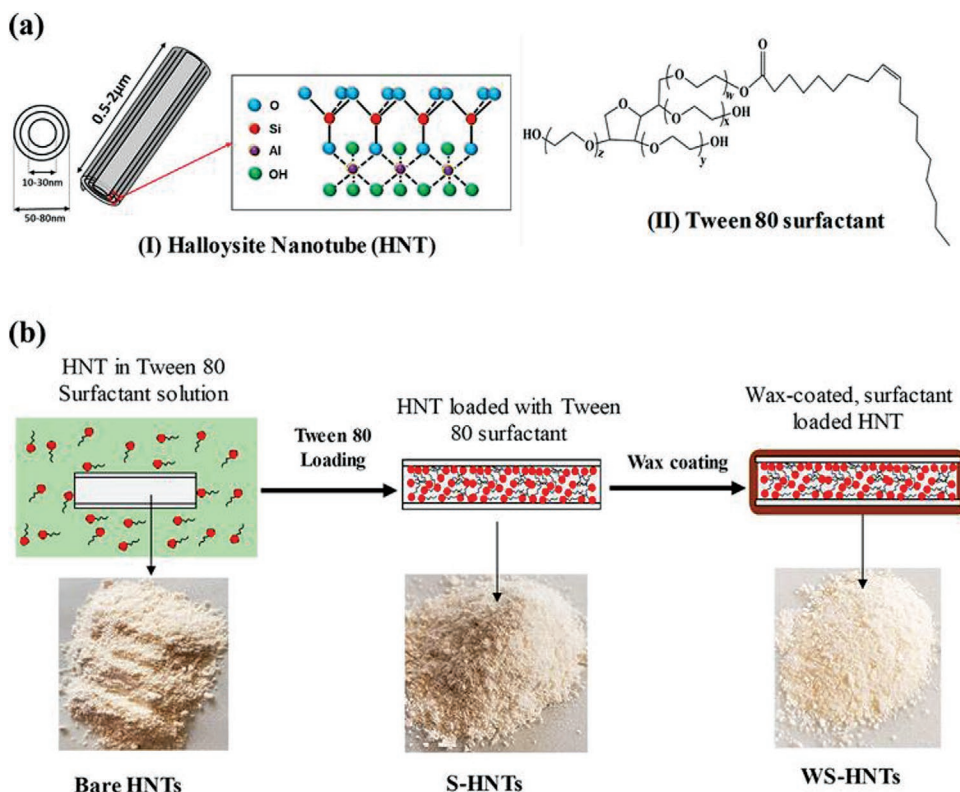


**Figure 10.** a) Chemical structure of halloysite nanotubes and Tween 80 surfactant. b) Scheme of the preparation steps for surfactant-loaded halloysite nanotubes coated with wax. Reproduced with permission.<sup>[161]</sup> Copyright 2020, American Chemical Society.

the effect of polypeptoid-grafted HNTs (g-HNTs) on the o/w emulsion stability, dodecane-in-water emulsions were prepared in artificial seawater (35 g L<sup>-1</sup> NaCl). The measurement of the Creaming Index enlightened the formation of highly stable systems when hydrophobic copolypeptides are coating the clay. Conversely, the CI showed that the emulsions containing the hydrophilic polypeptoid-grafted HNTs are unstable. In the former case (HLB = 12.0–15.0), the coalescence of Pickering emulsions is hindered and their mean diameters remain unchanged after 7 days, as a consequence of modified nanotubes attachment at the o/w interface and formation of an interconnected network.<sup>[164]</sup> Moreover, the study of the dynamic interfacial tension at the dodecane-saline water interface showed that it is correlated to the HLB of the grafted polypeptides, being lower when the polymer is more hydrophobic. The calculation of the energy of detachment, which was carried out by using experimentally derived contact angle values (ranging from 42 ± 5° to 146 ± 1° as the hydrophobic content of the polypeptides increased) indicated that the functionalization of halloysite deeply enhances its partition and anchoring at the oil/water interface, being ΔE<sub>det</sub> 26 times higher than that of bare clay and also higher the more hydrophobic is the stabilizer. The viscosity of the system was also studied by steady shear experiments of dodecane-saline water droplets stabilized by g-HNTs and it showed that, after functionalization, the viscosity increased compared to pristine halloysite thus contributing to the emulsion stability.<sup>[164]</sup> Besides, cell culture studies conducted on *A. borkumensis* showed that polypeptoid-grafted HNTs enhanced the maximum cell numbers in the culture, especially for halloysite functionalized with

more hydrophobic polypeptides. Since smaller emulsions can be formed with larger interfacial area compared with the bare clay stabilized system, this can also play a role in the increased cell growth rate. Hence, g-HNTs are green and biocompatible emulsifiers whose stabilizing efficiency is strongly influenced by the HLB characteristics of the grafted polypeptides and they are nontoxic toward the dominant hydrocarbon degrading bacteria but, rather, they can stimulate their growth thus optimizing the oil spill remediation.<sup>[164]</sup>

With regard to this, Panchal et al. investigated the proliferation of hydrocarbonoclastic bacteria on oil/seawater emulsions stabilized by pristine and ODTMS-modified halloysite.<sup>[166]</sup> As a first observation, no significant difference was reported in the growth rate and generation time of *A. borkumensis* in the marine broth supplemented with clay stabilized n-hexadecane or Macondo crude oil, meaning that halloysite is safe for the organisms even after modification. On the other side, the metabolic activity of bacteria increased in the presence of HNTs, indicating that the cells viability and ability to consume and convert nutrients is enhanced. The colonization of oil droplets with hydrocarbon-degrading microorganisms was observed using bright field optical microscope. By using n-hexadecane as unique source of carbon it was found that the addition of ODTMS-HNTs leads to the formation of a dense patterned biofilm of bacteria at the surface of the oil droplet after 5–7 days, as result of the bacterial growth between different nanotubes.<sup>[166]</sup> Most interestingly, the capability of *A. borkumensis* to proliferate on the surface of crude oil droplets was investigated and compared to the detergent-based technology (Figure 11).

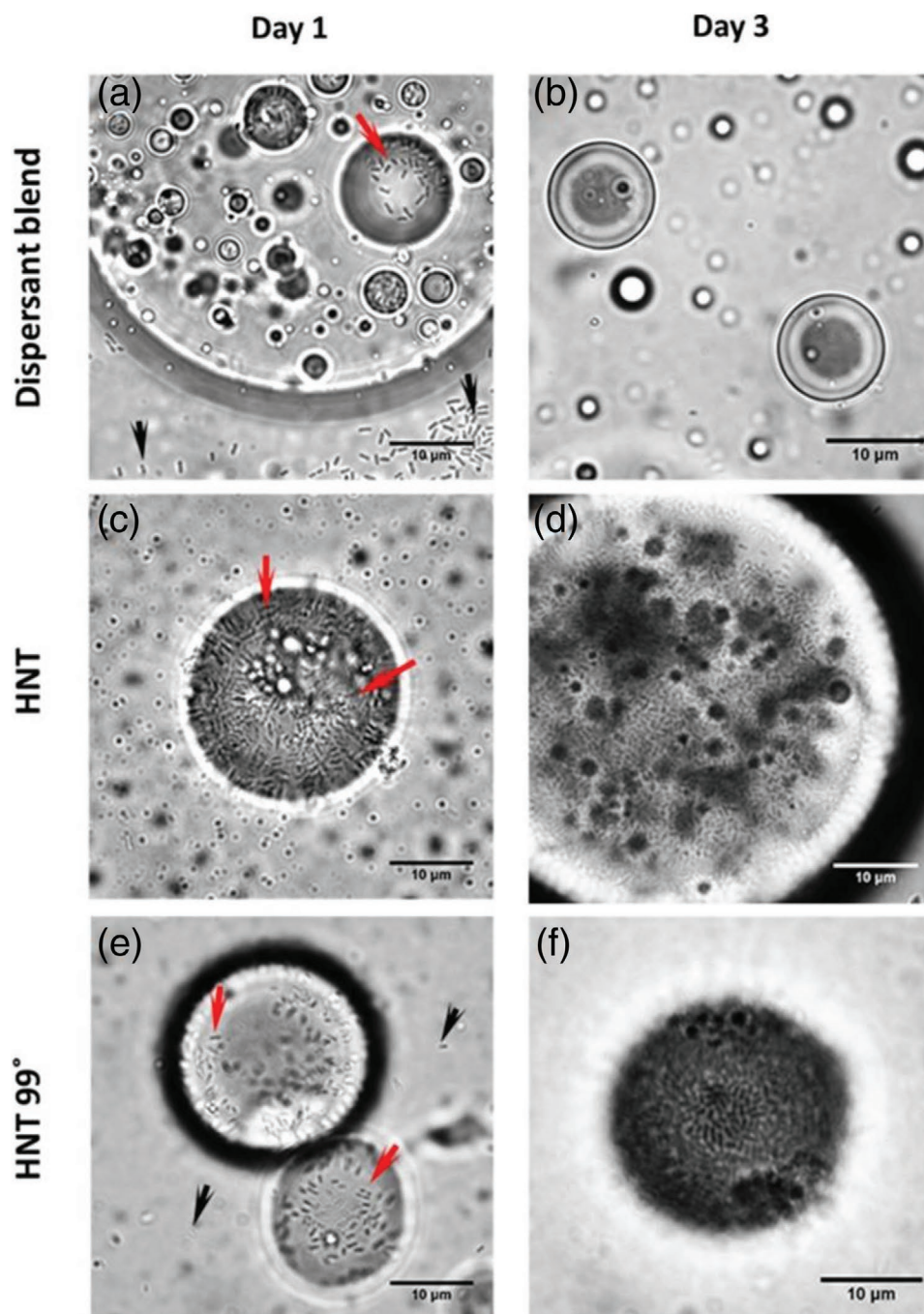


**Figure 11.** Optical microscopy images of crude oil emulsions formed with a,b) 1 wt% dispersant blend c,d), 1 wt% of pristine HNTs e,f) and 1 wt% of hydrophobized ODTMS-halloysite 1 and 3 days after inoculation of *A. borkumensis*, respectively. Reproduced with permission.<sup>[166]</sup> Copyright 2018, Elsevier Ltd.

It is possible to observe that a small number of rod-shaped cells are attached to the surface of droplets stabilized by the dispersant blend, which is composed by 48% non-ionic and 35% anionic surfactants representative of Corexit, both at 1 and 3 days from bacteria inoculation (Figure 11a,b). This effect can be most likely related to the repulsion between bacteria and the anionic species or to the growth inhibition of cells. Conversely, the proliferation on pristine halloysite stabilized emulsions

occurs immediately but no further increase can be observed after 3 days (Figure 11c,d), whereas the bacteria proliferation leads to the formation of a dense biofilm on ODTMS-halloysite coated crude oil droplets (Figure 11e,f).<sup>[166]</sup> Starting from these results, new perspectives to treat oil spill by bio-remediation have been opened.

For instance, reversing the structure of HNTs stabilized Pickering emulsions allowed to fabricate a new type of liquid

marbles possessing a high amount of microorganisms encapsulated within the spherical structure.<sup>[167]</sup> The growth of bacteria inside the marble, which is due to the hydrophobic modification of the clay, is responsible for the formation of a biofilm that improves the resistance of the material thus keeping the bacteria safe for a long period. This findings open up a new strategy for the storage of microorganisms and for the wastewater treatment.<sup>[167]</sup>

Literature also reports another method for the adsorptive removal of oily pollutants from water and it deals with the use mesoporous/macroporous HNTs based microparticles prepared by a Pickering templated-assisted approach.<sup>[168]</sup> Halloysite was firstly functionalized with chitosan to modify its charge and the hydrophobic behavior in order to enhance the attachment of the tubes at the oil/water interface. The design of the porous microstructures was carried out by anchoring the chitosan modified HNTs on SDS-stabilized ethyl acetate emulsions via electrostatic interactions and Pickering effect. It should be noted that SDS-coated surface is negatively charged whereas the chitosan-modified nanoclay is positively charged. The importance of charges and electrostatic interactions on the formation of Pickering emulsions was previously elucidated. Then, the pH was changed to favor the aggregation of droplets which furtherly overcome solvent diffusion and evaporation of ethyl acetate, washing and drying into the final porous materials. The capability of these materials to adsorb crude oil from water depends on several parameters, such as amount of adsorbent, contact time, temperature. The pH also plays a role because it can affect the interactions between the adsorbent and the adsorbate. In this case, the best condition was measured to be in the pH range between 5 and 6.9. Moreover, the oil droplets uptake decreased with the increasing ionic strength of the solution due to the screening effect of the surface charges. It is also reported that the crosslinked microparticles led to lower removal efficiency compared to non-crosslinked microparticles because of their smaller BET surface. The optimization of all these parameters resulted in the maximum removal of 94.5% of emulsified oil by the chitosan-grafted HNTs microparticles.<sup>[168]</sup>

It is worth to note that the self-settleability of an adsorbent is also crucial to its practical application because it makes easier the final separation of adsorbent-adsorbate complex after the water treatment. In this case, settleability studies showed that the chitosan-grafted HNTs microparticles display the highest self-settleability rate both in water (i.e., 83.53% in 30 min) and emulsified solutions (96.48% in 30 min). Besides, the adsorbent was regenerated by using a mixture of ethanol and hexane to wash out the adsorbed oil and it was possible to re-use it for five cycles with a minimal loss in performance. The high efficiency, self-settleability and ease of regeneration make these materials very promising for the treatment of water.<sup>[168]</sup>

Finally, Zhou et al. developed a water-compatible molecularly imprinted polymer via Pickering emulsion polymerization using halloysite nanotubes (HNTs@MIP) as stabilizing solid particles for the selective removal of 2,4-Dichlorophenoxyacetic acid (2,4-D) in aqueous media.<sup>[169]</sup> It is well known that MIPs are a class of functional materials prepared by the copolymerization and cross-linking of monomers with a template. After the removal of the template, some cavities are created each of them representing an adsorption site with high specificity.<sup>[170]</sup>

2,4-D was chosen because its wide use as herbicide raises several concerns related to water pollution, poor biodegradability, and moderate toxicity. Since the obtained HNTs@MIP displayed high selectivity, excellent recognition and rapid kinetic binding toward 2,4-D in water solution, it can be exploited for the adsorption and separation of a broad class of chemicals for environmental remediation.<sup>[169]</sup>

Besides the oil spill (bio-)remediation, HNTs based Pickering emulsions can also be employed for the enhanced oil recovery (EOR). In particular, literature reports the design of highly stable Pickering systems based on halloysite coated with glucose-based cationic nonionic surfactants which showed, as results of the nanofluid flooding test, a significant improvement of oil recovery efficiency and a good oil displacement effect.<sup>[171]</sup> Despite the development of ecofriendly sources, fossil fuels still represent the dominant energy resource in the global supply and the EOR based approaches are crucial to increase the productivity of oil wells with minor risks for the environment and the ecosystem.

#### 4.2. HNTs Based Pickering Emulsions for Catalysis

Nowadays, nearly 80% of chemical reactions are catalyzed. It is well known that homogeneous catalysis is a process displaying high selectivity, quantitative yield and an advantageous reaction path. However, several issues make the homogeneous catalysis complicated to be performed because of low recyclability, difficulty to separate products from catalyst, loss of the catalyst itself. Hence, heterogeneous catalysis represents a valid alternative. In this case, the phase of catalysts differs from that of the reactants or products and both recycling and separation are easier processes. The hydroformylation of olefins to aldehydes is one of the most important reactions for industrial applications and it can be heterogeneously catalyzed in a two-phase system by a rhodium (Rh) based catalyst.<sup>[172]</sup> Being this reaction conducted in water, it is limited only to short-chain olefins who display enough water solubility compared to the hydrophobic long chain olefins. The latter, indeed, must still be hydroformylated in a homogeneous phase, with all the problems related to the loss of the metal, which is very precious and expensive.<sup>[172]</sup>

In this context, Pickering emulsions shown to be efficient in interfacial catalytic reactions and can overcome these limitations.

von Klitzing et al. reported the hydroformylation of long chain olefins to aldehydes, namely dodecene to tridecanal, by halloysite stabilized emulsions.<sup>[173]</sup> Firstly, the structure of the resulting emulsions was tailored by changing some experimental conditions such as concentration of the clay, vortexing time during preparation, degree of hydrophobization, length of the nanotubes and salinity of the medium. It was found that for emulsions with 0.5–1 wt% in halloysite, the size of droplets is lower as the vortexing time increases from 1 to 3 min and the length of nanotubes does not affect the average diameter of Pickering emulsions. In this case, the distribution of the droplets dimensions can be influenced, being narrower as the tubes are longer and it can be most likely related to a higher steric hindrance which prevents emulsions aggregation and the formation of larger droplets which would constitute

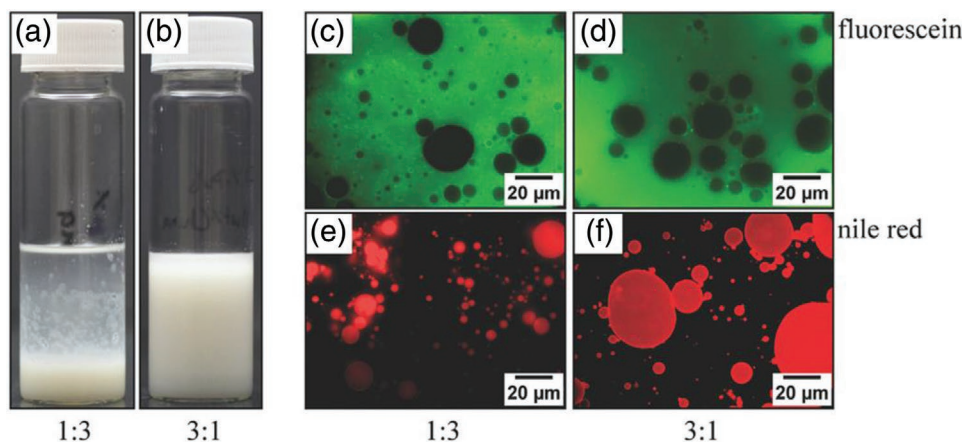


**Figure 12.** a,b) Images of halloysite stabilized emulsions at the mass ratios of 1:3 and 3:1. (c,f) Fluorescence microscope images of the emulsions. c,d) The water phase was dyed with fluorescein, and e,f) the dodecene phase was dyed with Nile red. c,e) Water to oil mass ratio of 1:3, (d,f) water to oil mass ratio of 3:1. Reproduced with permission.<sup>[173]</sup> Copyright 2016, WILEY-VCH.

the distribution tail. Also, an increase in halloysite concentration leads to denser packing at the oil/water interface of laterally oriented nanotubes, which stabilize the droplets against coalescence. In order to study the effect of ionic strength and hydrophobicity, studies were conducted in pure water and NaCl aqueous solutions, simulating seawater, by using pure, Hexamethyldisilazane (HMDS) and octadecyltrimethylsilazane (ODTMS) modified HNTs. It was found that the dimensions of droplets decreased in the presence of salt, due to the screening of electrostatic repulsions between nanotubes and to a denser packing at the interface. For what concerns the modified clays, instead, salt does not play a role on the interactions but the use of halloysite with the highest hydrophobic behavior (ODTMS-HNTs) leads to smaller droplets compared with HNTs possessing medium hydrophobization (HMDS-HNTs).<sup>[173]</sup>

In order to perform the hydroformylation of olefin, 1-dodecene was used as reactant and oil phase in the Pickering emulsions stabilized by pristine halloysite. The catalyst precursor was  $[\text{Rh}(\text{acac})(\text{CO})_2]$  modified with a water soluble ligand. The reaction was conducted in a multiphase system. **Figure 12** shows that, regardless of the water/dodecene ratio, the prepared Pickering emulsions were always oil-in-water type.

Fluorescence microscopy images show that both fluorescein dyed emulsions (Figure 12c,d) and Nile red dyed emulsions (Figure 12e,f) are formed by oil droplets dispersed in the water phase for 1:3 and 3:1 water:oil mass ratios. It was also possible to observe that the oil phase is not completely dispersed in the water phase for 1:3 ratio and, contrarily to it, it becomes homogeneously dispersed for 3:1 ratio, without any visible excess of dodecene (Figure 12a,b).

The results of the catalyzed hydroformylation of 1-dodecene to tridecanal showed that after 24 h more than 36 wt% of the product was formed and the amount of by-product (i.e., isoaldehyde) remains negligible during the whole reaction. Hence, the selectivity is very high and the catalyst in the water phase can be easily recovered by membrane filtration after the reaction without any consequences on the oil phase. These are the most outstanding advantages in the use of Pickering emulsions for catalytic purposes: the combination of the high selectivity and high activity, typical of the homogeneous catalysis, with the

efficient separation and easy recyclability proper of the heterogeneous catalysis.<sup>[173]</sup>

Also, Stehl et al. investigated the effects of the Rh based catalyst on the energy of detachment, droplets size and stability of halloysite based Pickering emulsions and they focused on the influence of these parameters also on the hydroformylation of 1-dodecene.<sup>[174]</sup> It is reported that the presence of the catalyst is responsible for a time-dependent decrease of oil/water interfacial tension from 50 to 14  $\text{mN m}^{-1}$  after 20 min due to its molecular adsorption at the interface. Interestingly, the variation of the energy provided to homogenize the components of the Pickering system also affects the final result. For instance, preparing the emulsions by high energy sonication leads to the formation of oil-in-water nanometric droplets without particles attached at the interface, given the too high curvature. Contrarily to it, the employ of ultraturrax (UT) with a lower energy input results in micrometric particles which display HNTs attached at the external interface. Therefore, UT was preferred to ensure the anchoring of solid stabilizers to the droplets, whose diameter monotonously decreased with increasing the clay concentration. Being the three phase contact angle of HNTs = 30°, the energy of detachment was calculated to be 34 192 kT. The further addition of the Rh-based catalyst to the water phase caused a slight reduction of  $\Delta E_{\text{det}}$  to 25 009 kT, as a consequence of the decrease of the contact angle. Nevertheless, in the case of HNTs stabilized emulsions with the addition of the catalyst, the highest mechanical stability was observed. This finding can be related to the higher coverage degree and to the attractive capillary forces between nanotubes, which lead to self-assembled bundles.

For what concerns the hydroformylation, instead, pristine HNTs-stabilized Pickering emulsions prepared by low energy input (UT) leads to a low conversion of 1-dodecene to tridecanal (i.e., 13 wt%, TOF = 18  $\text{h}^{-1}$ ). In comparison, Pickering emulsions prepared by high energy input (sonication) show an increase in conversion due to the smaller droplets size and to the absence of particles at the interface which interrupt the contact between the catalyst and the oil. However, both the preparation protocols resulted in low amounts of by-products in the oil phase and they display high selectivity. These factors, together with absence of leaching or loss of catalyst and ease



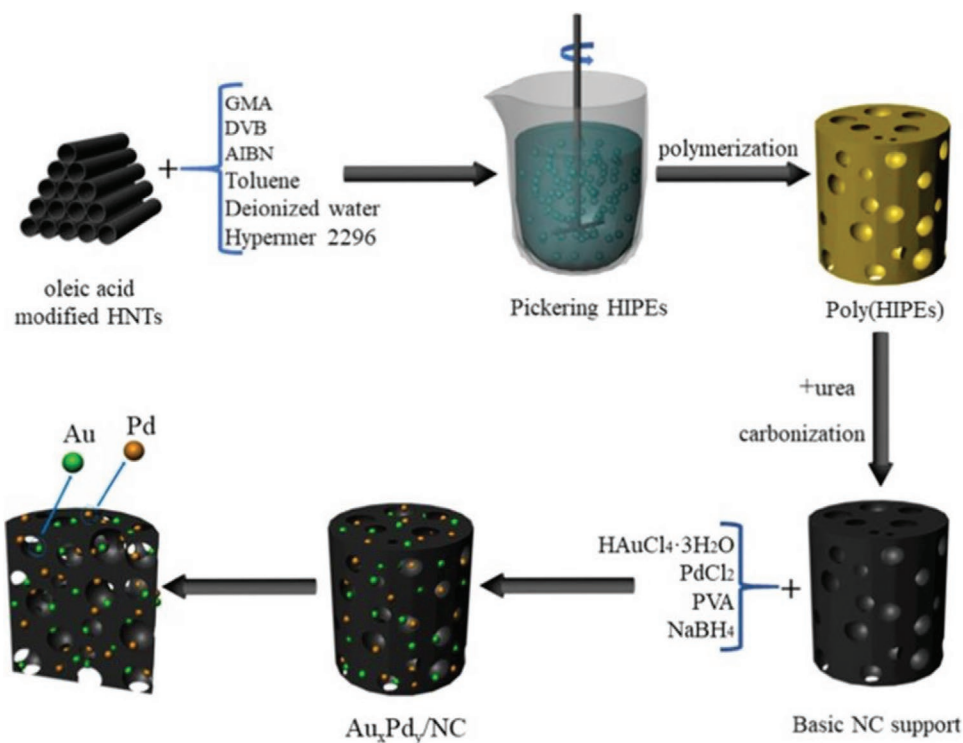


**Figure 13.** Preparation scheme for Pickering HIPEs derived hierarchical porous nitrogen-doped carbon supported bimetallic AuPd catalyst. Reproduced with permission.<sup>[175]</sup> Copyright 2020, Elsevier Ltd.

of separation and recycling, make convenient the use of Pickering emulsions which, still, combine the advantages of homogeneous and heterogeneous catalysis.<sup>[174]</sup>

Finally, Guan et al. reported a versatile strategy based on halloysite stabilized Pickering high internal phase emulsions (Pickering HIPEs) for the preparation of a hierarchical porous nitrogen-doped carbon (NC) supported bimetallic AuPd catalyst to be exploited for the selective aerobic oxidation of biomass derivative 5-hydroxymethylfurfural (HMF) into high value-added 2,5-furandicarboxylic acid (FDCA).<sup>[175]</sup> Pickering HIPEs are usually referred to as super-concentrated emulsions stabilized by solid particles with a minimum internal phase volume fraction.<sup>[176]</sup> The aim to find an advantageous path to perform this specific catalytic reaction is crucial in order to join together the increasing societal need for energy and the compelling demand for a green and sustainable development model to decrease the environmental impact. HMF is a biomass derivative with similar chemical properties with terephthalic acid (TPA). It is well known that the esterification of TPA leads to the preparation of polyethylene terephthalate (PET), which is one of the five major engineering petroleum-based plastics.<sup>[177]</sup> In this context, the preparation of FDCA would provide a renewable and eco-friendly polymer with better thermal stability and mechanical performances than PET. As a consequence, the former could replace the latter and the selective oxidation of HMF to obtain FDCA has attracted extensive attention. However, this reaction requires noble metals as catalysts and an alkaline medium, which represents several issues due to its corrosive activity and pollution.<sup>[178]</sup> The employ of nitrogen-doped carbon supports allows to overcome this limitation because the

electron-rich properties of nitrogen promote the formation of base sites on the catalyst surface, avoiding the addition of alkaline solvents. The interaction between carbon nitride carriers and the active substances improves the overall stability of the catalyst.<sup>[179]</sup> **Figure 13** reports the preparation route.

Oleic acid modified HNTs were used as solid stabilizers for Pickering HIPEs possessing toluene as oil phase. Then, porous Poly(HIPEs) were obtained by thermal initiating radical polymerization. The addition of urea and further carbonization allowed to prepare the porous nitrogen-doped carbon (NC) support with hierarchically microporous, mesoporous, and macroporous morphology. In this case, the presence of Hypermer 2296 surfactant as co-emulsifier in the starting mixture is responsible for the connection between pores in an open cell structure. Finally, the bimetallic Au/Pd catalyst was loaded onto the carrier, thus leading to the formation of the Au<sub>x</sub>Pd<sub>y</sub>/NC system.<sup>[175]</sup> It is worth to note that any variation in the urea content affects the nitrogen doping and changing the amount of AuPd metal gives raise to different loadings. Bearing the NC support some base sites, the reaction can be conducted without any alkaline addition. Most importantly, some synergistic effects arise from the combination of the support and the bimetallic centers.

The study of the catalyzed oxidation of HMF to FDCA using molecular O<sub>2</sub> as an oxidant was conducted by evaluating the effect of several parameters such as reaction temperature, reaction time, oxygen pressure, Au/Pd mass ratio, catalyst dosage and basicity of catalyst support. It is demonstrated that the optimal conditions are 140°C, 12 h, 2.0 MPa O<sub>2</sub>, 60 mg Au<sub>0.5</sub>Pd<sub>0.5</sub>/NC catalyst. In this case, increasing the basicity of

NC did not increase the yield, which remains similar to that one reached with a NC support showing mild alkaline character.

The results of conversion efficiency were very promising: the highest yield of 96.7% FDCA was achieved under these optimal reaction conditions. Furthermore, regeneration test revealed that the obtained  $Au_xPd_y/NC$  catalyst can be recovered and reused five times without significant loss of catalytic activity.<sup>[175]</sup> The green and environmentally friendly biomass conversion can be carried out starting, here again, from the preparation of Pickering emulsions to design a versatile and efficient nitrogen-doped carbon supported base-free bimetallic catalyst.

Also Chen et al. used a Pickering high internal phase emulsion as template for the design of a bifunctional catalyst to be exploited for the synthesis of 5-ethoxymethylfurfural (EMF) from biomass derivatives. They reached high yields of EMF in optimal reaction conditions in an ethanol/tetrahydrofuran (THF) medium.<sup>[180]</sup>

### 4.3. HNTs Based Pickering Emulsions for Health Applications

The self-assembly of nanoparticles at liquid–liquid interfaces is a powerful tool that offers a straightforward pathway for the production of organized nanostructures to be exploited in a wide range of applications. As it was previously mentioned, the design of Pickering emulsion holds a certain importance even for health related applications and technologies.

For instance, Wei et al. reported the preparation of ibuprofen loaded poly(lactic-co-glycolic acid) (PLGA) microparticles by exploiting the formation of Pickering emulsions and solvent volatilization.<sup>[181]</sup> To do it, stable oil-in-water droplets were formed using HNTs attached at the oil/water interface, being the oil phase a dichloromethane ( $CH_2Cl_2$ ) solution of PLGA. Then, halloysite coated PLGA microparticles were fabricated by the evaporation of  $CH_2Cl_2$  from the core of emulsions. **Figure 14a,b** shows that these microparticles are completely coated by nanotubes, as confirmed also by EDS analysis where Al and Si peaks can be found, which are proper of halloysite (**Figure 14d**).

Also, bare PLGA microparticles were reached after washing the HNTs coated precursor with an acid aqueous solution composed of HF and HCl, which can dissolve the nanoclays. They preserve the spherical shape and possess a smooth surface after the removal of the inorganic solids, which is confirmed by the lack of Al and Si in the EDS spectra (**Figure 14e,f,h**). As final step, the encapsulation of ibuprofen into the PLGA microparticle was studied by dispersing it in the  $CH_2Cl_2$  solution of the polymer during the first preparation step. Herein, it is reported that the pH of the solution affects the loading efficiency of the drug due to its protonation and deprotonation, which vary the solubility. Similarly, the release kinetics of ibuprofen from PLGA microparticles depends on pH and at pH = 7.4 it is faster compared to pH = 1.2. However, because of the barrier effect of the polymeric matrix, some drug remains entrapped within the microparticles and could be released only upon the disintegration of PLGA. Fitting the profiles allowed to assess that the release follows Fickian diffusion. It should be noted that the reported structure is biodegradable, no molecular surfactants are employed and PLGA is the only polymer used in the whole

procedure.<sup>[181]</sup> This is an important point because PLGA is certified by the Food and Drug Administration (FDA, USA) as safe component in many health related fields from orthopedics to tissue engineering, from drug carriers to delivery systems.<sup>[182]</sup>

Literature also reports another example of the employ of halloysite stabilized Pickering emulsions for the preparation of porous materials to be used in health applications. For instance, Hu et al. developed a class of poly(L-lactic acid) (PLLA)-modified halloysite nanotubes (m-HNTs)/poly( $\epsilon$ -caprolactone) (PCL) porous scaffolds by solvent evaporation of water-in-PCL clay stabilized droplets, which acted as templates.<sup>[183]</sup>

The characterization of PLLA-HNTs allowed to confirm that the grafting and the hydrophobic modification of the nanotubes occurred. The amount of PLLA-COOH was found to be 3.45 wt%. For what concerns the m-HNTs stabilized Pickering emulsions having a  $CH_2-Cl_2$  suspension of PCL as oil phase, they can be easily dispersed in dichloromethane but they aggregate in water. As a result, their water-in-oil nature was also confirmed and they could be stored for about 1 month at room temperature due to the high stability. Similarly to the previously reported studies, the emulsions were smaller and more stable as the clay concentration increased, due to the higher coverage of the W/O interface and to the steric hindrance which prevents collision and coalescence. Also, increasing the water to oil volume ratio created destabilization because the m-HNTs were not enough to cover the larger water–oil interfacial area of the emulsions droplets, which tended to collide and coalesce.

As a consequence, tuning these parameters (i.e., m-HNTs concentration, W/O volume ratios) allows to tailor the pores dimension of the final m-HNTs/PCL scaffolds from several dozen micrometers to over one hundred micrometers, depending on the diameter of Pickering emulsions templates before solvent evaporation. Since the bacterial infection can be detrimental in the initial period of the scaffold implantation, the antibacterial drug enrofloxacin (ENR) has been loaded into the scaffolds. For this aim, ENR was dispersed in the oil phase and the same preparation protocol was followed. The direct solvent evaporation allowed to reach high loading efficiencies, ranging from  $97.8 \pm 3.6\%$  to  $98.5 \pm 3.9\%$ . The study of the release kinetics displayed a burst release in the initial 12 h and a sustained release in the following 150 h.<sup>[183]</sup> Most interestingly, the release rate increases for m-HNTs/PCL scaffold possessing higher drug amounts and it is slower for less porous samples. In this case, the use of higher amounts of halloysite during the preparation is responsible for smaller pores diameters and the ENR remains entrapped for longer time. Moreover, the inhibition zone method was used to evaluate the antibacterial activity of the drug loaded scaffolds against *E. coli* (**Figure 15**).

It is clear that the control sample without any ENR loading has no antimicrobial activity. Contrarily to it, the ENR-loaded scaffolds formed a visible dark ring around them, proving their excellent capability in inhibiting the growth of *E. coli* even after 192 h (**Figure 15a–c**). It is noteworthy that, after 40 h, the inhibition ring is larger for the scaffold  $M_{75}E_5$  compared to the others, as a consequence of the higher amount of drug loaded into its pores (**Figure 15d**). Finally, in vitro cell culture assay was carried out to assess the biocompatibility of the m-HNTs/PCL porous scaffold by seeding mouse bone mesenchymal stem cells (mBMSCs). **Figure 15e** reports the proliferation ability of

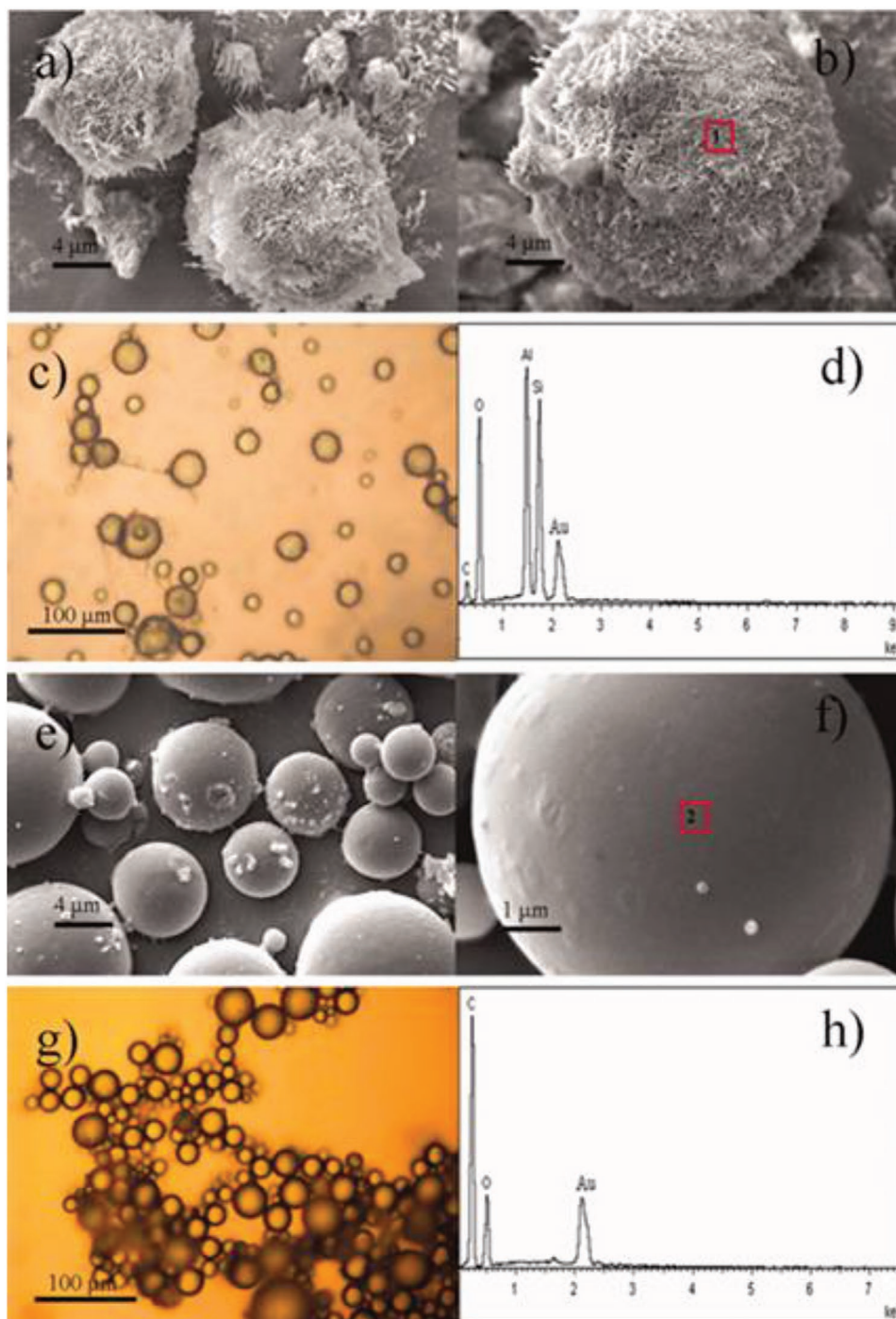


**Figure 14.** SEM images of a,b) HNTs-coated PLGA microparticles, e,f) bare-PLGA microparticles. d,h) EDS spectra of the hybrid microparticle and bare-PLGA microparticle at areas in red squares in images (b) and (f), respectively. c,g) Optical microscopy images of HNTs-coated PLGA microparticles and bare-PLGA microparticles, respectively. Reproduced with permission.<sup>[181]</sup> Copyright 2012, Wiley Periodicals, Inc.

cells, here described as optical density (OD), as a function of time after 1, 3, and 5 days after implantation in scaffolds with different m-HNTs concentrations. It can be assessed that the mBMSCs can survive and proliferate. Interestingly, the adhesion and proliferation of cells was enhanced by increasing the amount of HNTs into the PCL matrix due to the higher surface roughness.

In conclusions, the m-HNTs/PCL scaffolds possess tunable morphology, they have long term antimicrobial properties and they are also cytocompatible. All these features demonstrate their great potential in tissue engineering and drug carriers applications.<sup>[183]</sup>

In their work, Li et al. exploited the capability of halloysite nanotubes to attach at the interface, known as “Pickering effect”,

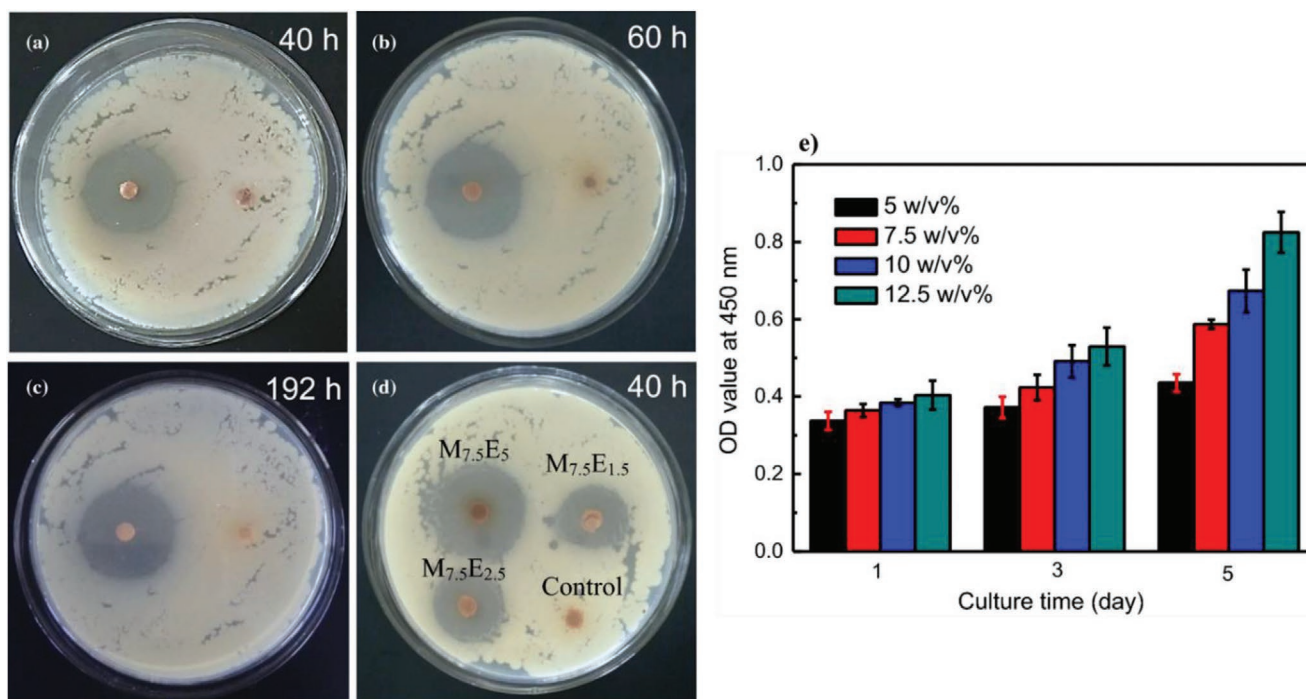


**Figure 15.** Antibacterial activities of ENR-loaded scaffolds with different storage times against *E. coli*: a) 40 h, b) 60 h, and c) 192 h. d) Antibacterial activities of ENR-loaded scaffolds with the storage time of 40 h against *E. coli*. e) Cell proliferation of BMSCs after 1, 3, and 5 days of culture on the m-HNTs/PCL porous scaffolds with different m-HNTs concentrations. Reproduced with permission.<sup>[183]</sup> Copyright 2018, Springer.

to develop a biomimetic nanocarrier platform for target-specific delivery of phototherapeutic agents.<sup>[184]</sup> To do it, HNTs were firstly coated with poly(sodium-p-styrenesulfonate) (PSS) to enhance their biocompatibility and, then, their lumen was loaded with the type-II photosensitizer indocyanine green (ICG). ICG is a therapeutic agent for phototherapy, recognized and approved by the US Food and Drug Administration, which can be activated by near-infrared (NIR) irradiation to produce singlet oxygen and thermal effects against specific tumor cells.<sup>[185]</sup> The inhibition of cell proliferation via damaging of vital cell components including membranes, proteins and DNA is crucial for the development of phototherapy, as a valid alternative to chemotherapy and radiotherapy, in a non-invasive treatment of cancer. **Figure 16** reports the different steps of this work.

After decorating HNTs with PSS, the encapsulation of ICG within the lumen of the clay was driven by electrostatic attractions. It is reported that, upon 808 nm laser irradiation of the HNTs-PSS-ICG, the nanocarriers show enhanced efficacy of single oxygen photosensitization compared to pure ICG and the yield became even higher in aqueous medium or PBS buffer compared to organic solvents such as ethanol or DMSO.<sup>[184]</sup>

The photodynamic behavior of the nanocarriers was investigated after the attachment at the membrane of giant unilamellar vesicles (GUVs) via Pickering effects. Upon NIR irradiation, pristine clay had no effects and they showed biosafety. For what concerns the HNTs-PSS-ICG, instead, an advanced membrane disintegration was observed after 20 s, proving the high photodynamic therapeutic performance of the nanocarriers in oxidative membrane destruction. Aimed at investigating the cytotoxicity of the designed material against human breast cancer cells, the HNTs-PSS-ICG nanocarriers were further coated with MDA-MB-436 cell membranes to improve their biocompatibility

and to endow them with target specificity in the therapy performance owing to the inherent antigens in the membrane. After the incubation of the MDA-MB-436 cells, which are human cervical carcinoma tumor cells, with HNTs-PSS-ICG it could be observed that the nanocarriers adsorbed on the cells surface by membrane adhesion. In vitro studies of the phototherapeutic performance showed that after 160 s of NIR irradiation, the cancer cells membranes were significantly damaged whereas their nucleus overcome little morphological variation. The cell mortality reached a value up to 95%. Therefore, it is possible to assess that the designed nanocarriers exhibit high therapeutic effect in killing cancer cells by specifically targeting the membrane, due to their coating, rather than the nuclei.

Also, in vivo phototherapy studies were performed with tumor-bearing mice, which were subjected to tail intravenous injection of the membrane-coated HNT-PSS-ICG nanocarriers. Results showed a higher photothermal effect at the cancer site of mice compared with the injection of free ICG or uncoated HNT-PSS-ICG, under a safe irradiance of 300 mW cm<sup>-2</sup> at 808 nm. The phototherapeutic treatment resulted in a reduction of the tumor volume by a combination of photodynamic and photothermal effects upon near-infrared light exposure. It is possible to conclude that the HNT-PSS-ICG nanocarriers can specifically adsorb and attach at the interface of the cancer cells via Pickering effect and, once there, perform their excellent phototherapeutic activity.<sup>[184]</sup>

#### 4.4. HNTs Based Pickering Emulsions for Cultural Heritage

The consolidation and protection of cultural heritage represents one of the most compelling challenges of our time. The need to restore and protect the historical artifacts in order to bequeath

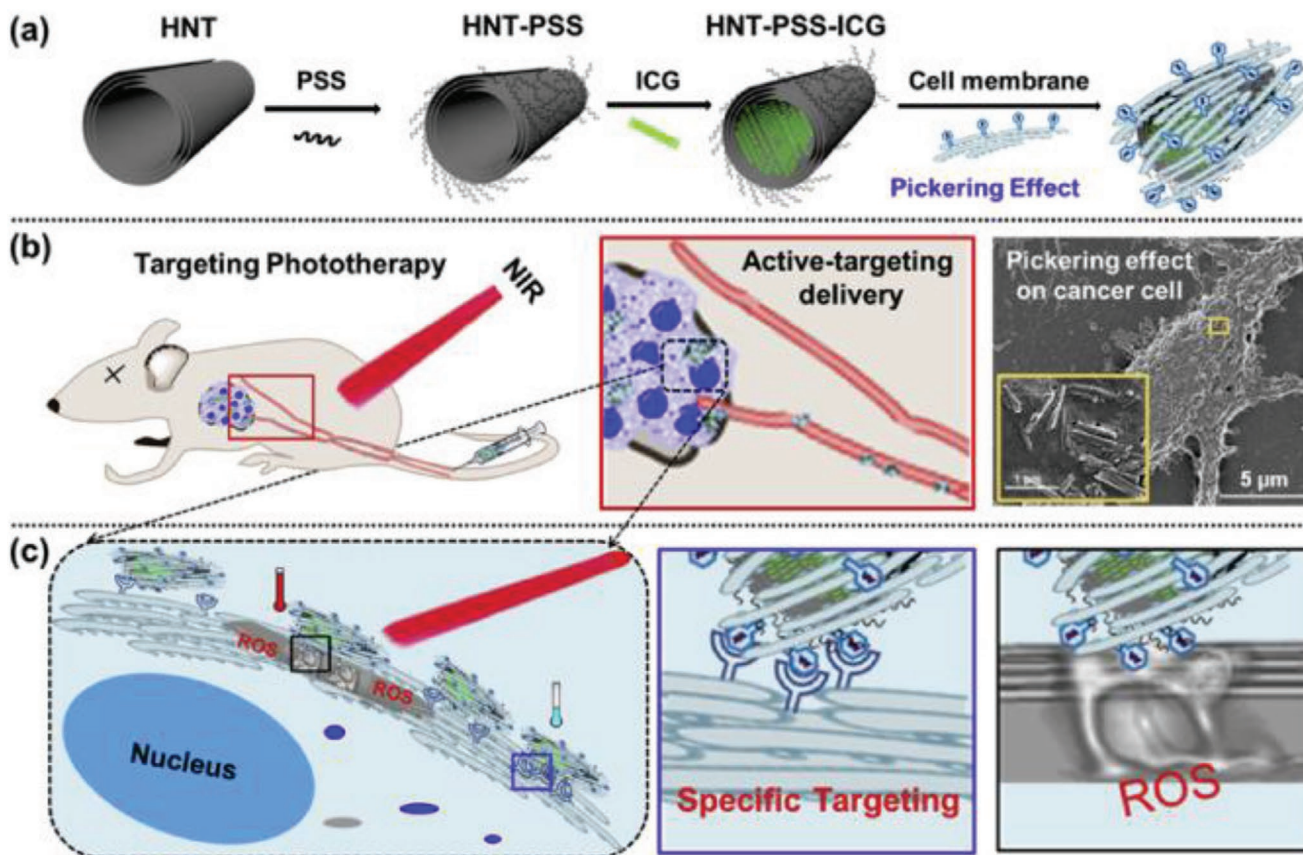


**Figure 16.** Schematic illustrations of a) the preparation of membrane-coated HNT-PSS-ICG nanocarrier, b) targeting phototherapy in model mice injected via tail vein with membrane-coated HNT-PSS-ICG nanocarriers and Pickering effect on cancer cell membrane, and c) specific targeting effect of membrane-coated HNT-PSS-ICG nanocarrier on cell membrane and cell disruption under NIR light irradiation. Reproduced with permission.<sup>[184]</sup> Copyright 2019, Elsevier Ltd.

them to the future generations as evidence of the past is crucial and it requires the commitment of scientists, restorers, historians and technicians. Pickering emulsions can play a proper role also in this field.<sup>[186]</sup>

It is well known that conventional surfactants stabilized emulsions are widely used in cleaning protocols given their ability to remove hydrophobic species from the surface of artworks by entrapping them into their core, in the case of oil-in-water droplets. Nevertheless, the uncontrolled spreading and penetration of these formulations can cause serious damages. The need to find alternative stabilizers, such as solid particles, arises in this context.

Cavallaro et al. designed a Pickering emulsions system based on halloysite and on a renewable biopolymer, namely pectin, for the removal of wax from marble surfaces.<sup>[187]</sup> To do it, HNTs stabilized oil droplets were prepared in a pectin aqueous solution and the addition of divalent cations allowed to increase the viscosity of the medium and to create a gel-like phase around them. In particular, the presence of the biopolymer in a gel-like phase can affect the stability and the dimensions of the Pickering emulsions.

Contrarily to chitosan, whose effect was also investigated in this work, which is responsible for phase separation, the employ of pectin provides further stabilization to the system. Indeed, oil droplets are homogeneously dispersed in the pectin

gel phase and the droplet size distribution is shifted toward smaller values compared to oil/HNTs/water Pickering emulsions. The calculation of the energy of detachment, which is  $70 \times 10^4$  kT for oil-in-water and  $125 \times 10^4$  kT for oil-in-pectin aqueous solution Pickering emulsions respectively, suggested that halloysite is strongly bonded and the presence of pectin enhanced the HNTs affinity toward the oil-water interface being  $\Delta E_{\text{det}}$  one order of magnitude higher. Also, the shelf life of the pectin Pickering emulsions gel was estimated to be 3 months. These effects are most likely related to the variation of interfacial tension, contact angle, and viscosity.<sup>[187]</sup>

Afterward, the ability of the Pickering emulsions in the pectin gel to remove wax from marble surfaces was investigated. The choice of wax is crucial because it is a good model system for hydrophobic layers on historical artworks and it was used in the past as a protective coating. Nowadays, its removal represents the first issue to handle during cleaning protocols.<sup>[188]</sup>

At first, the wax removal efficiency was studied by both colorimetric analysis and contact angle experiments after the application on a common piece of marble. It was found that HNTs based Pickering emulsions in the gel-like phase are able to remove the hydrocarbon species and the efficiency increases as a function of the contact time between the solid substrate and the cleaning formulation.<sup>[187,189]</sup> In particular, the marble surface is free of

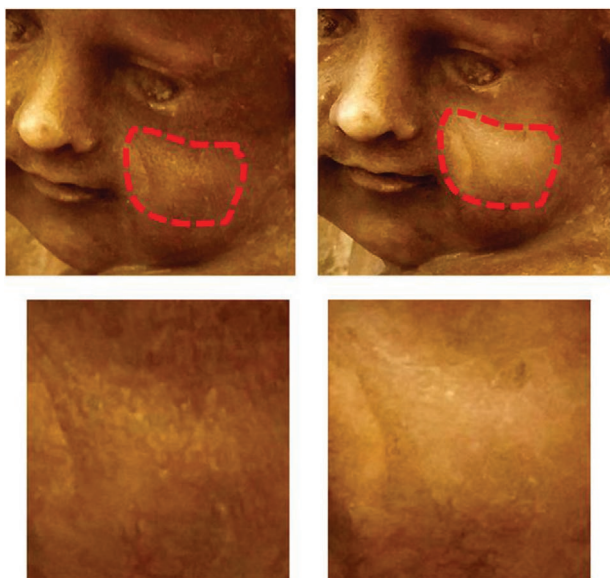


**Figure 17.** Application of the Pickering emulsion in pectin gel system on cherubs of the funeral monument of Placido Caruso (Polizzi Generosa, Italy): before cleaning (left) and after cleaning (right). Reproduced with permission.<sup>[187]</sup> Copyright 2019, American Chemical Society.

hydrophobic substances after  $\approx 50$  min long application time. It is noteworthy that no pectin residues can be found on the treated material after a proper water rinsing. Finally, the cleaning formulation was tested on a real artwork: the cherubs of the funeral monument of Placido Caruso from St. Joseph's Chapel in Polizzi Generosa (Italy). Results are reported in **Figure 17**.

Although the nature of the coating layer was unknown, it was composed by hydrophobic species as suggested by inefficient water cleaning. Here, the employ of the designed formulation made of halloysite stabilized Pickering emulsions in the gel-like pectin phase resulted in a controlled cleaning process of the surface, which appears whitened after 10 min long contact time. Therefore, the designed system is very promising for cultural heritage related applications, especially for marble or stone based artworks. The presence of a gel provides an easier manageability of the formulation, which can be swabbed in a controlled area without spreading away. Besides, except for the oil phase, all the components are green, eco-sustainable and they are obtained from natural resources.<sup>[187]</sup>

Within the field of cultural heritage treatment, the conservation of waterlogged archeological woods represents another issue to tackle. After several centuries under water or anoxic environments, the wooden structure loses mechanical resistance due to the degradation of lignocellulosic polysaccharides and lignin carried out by bacteria and fungi.<sup>[190]</sup> As a consequence, their recovery is a critical problem because the artworks can collapse and be destroyed upon drying before being treated and exposed in museums or exhibitions.

In the recent times, several procedures have been developed and the most common ones deal with the use of poly(ethylene) glycols (PEGs). This method was very promising at the beginning, since it allowed to reinforce the structure of the waterlogged woods with high efficiency in the short term. However, later, some detrimental consequences

were enlightened.<sup>[191]</sup> For instance, the interactions between PEGs polymeric chains and sulfate or iron compounds in the woods are responsible for the production of acidic species which increase the acidity inside the wooden structures, thus enhancing the degradation in the long term.<sup>[192]</sup> The damage of Vasa, a Swedish warship from the 17th century, is the most popular example.<sup>[193]</sup>

Other methods dealing with the use of biopolymers, ethers, sugars, epoxy resins, or inorganic species are also critical due to the need for high amounts of either organic solvents or acids or they alter the aspects of the artworks in the long term.<sup>[194,195]</sup>

In our previous work, we designed a novel protocol for the consolidation and protection of waterlogged archeological woods starting by the preparation of halloysite stabilized Pickering emulsions possessing paraffin wax as inner core.<sup>[196]</sup> Herein, the formation of oil-in-water droplets with nanotubes at the interface was reached by exploiting the thermal properties of wax, which is solid at room temperature and turns into liquid upon heating. After melting, paraffin catches the clay around the droplets and solid wax microparticles with halloysite entrapped at the outer surfaces can be created after cooling down. **Figure 18** reports the SEM images as a function of halloysite content.

It can be observed that halloysite nanotubes are attached at the external surface of the Pickering emulsions, whose coverage degree depends on the clay concentration during the preparation procedure, and it is higher as the amount of HNTs increases. Moreover, as reported for others Pickering systems, the particles are smaller when more solid stabilizers are anchored at the interface. In order to study the effect of halloysite on the crystallinity of the paraffin and to have insights about the thermodynamics of wax melting, micro differential scanning calorimetry ( $\mu$ -DSC) experiments were carried out. It was found that, despite the transition temperature did not change after the addition of clay compared to the pure hydrocarbons, the enthalpy of the process ( $\Delta H_m$ ) decreased. This finding is most likely due to the partial loss of crystallinity by paraffin because of the nanoparticles anchoring at the outer surface.<sup>[196]</sup>

Then, the designed microparticles were exploited for the treatment of waterlogged archeological woods. After the impregnation into wax/HNTs Pickering emulsions system, both the transversal and the radial section of the woods were coated by the wax/HNTs microparticles and the channels were filled, contrarily to untreated samples who displayed empty channels. It is worth to note that the treatment did not affect colorimetric properties of the consolidated materials.

The evaluation of the mechanical properties was carried out by dynamic-mechanical analysis (DMA). **Figure 19a** shows a preliminary macroscopic assessment.

It is clear that the consolidated wood gained robustness and mechanical resistance compared to the untreated sample, which is very fragile.

For what concerns the analysis of stress versus strain curves (**Figure 19b**), the results confirm that the treated wooden artworks possess higher mechanical resistance, rigidity and stiffness as showed by the enhancement of Young modulus and stress at breaking point. Therefore, due to their dimensions, the wax/HNTs microparticles can enter the wooden structure by filling the empty pores, thus avoiding the collapse and the

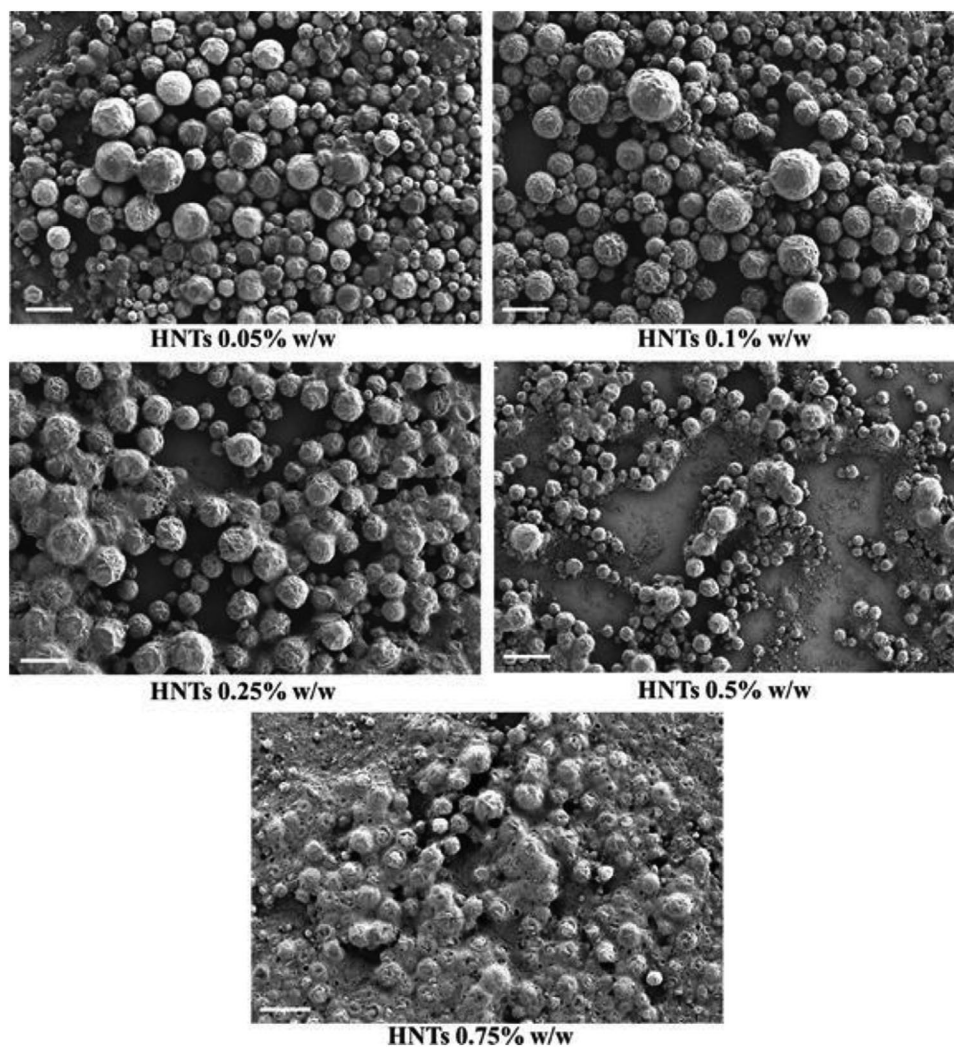


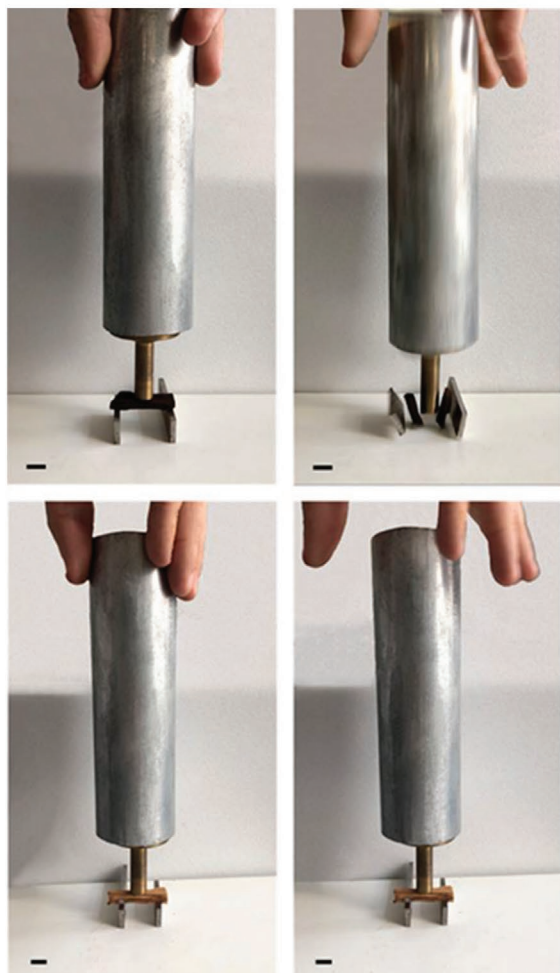
**Figure 18.** SEM images of wax/HNTs Pickering emulsions with increasing concentration of halloysite. Scale bars are 60  $\mu\text{m}$ . Reproduced with permission.<sup>[196]</sup> Copyright 2021, American Chemical Society.

loss of the material structure. Besides the remarkable results on the properties of the waterlogged archeological woods, one of the most important features of the proposed treatment protocol is its eco-friendliness. Water is the only solvent used throughout the whole procedure, no organic volatile solvents are employed, and this factor opens new perspective about the possibility for this method to be scaled up for the treatment of shipwrecks of larger dimensions.<sup>[196]</sup>

Afterward, starting from the preparation of wax/HNTs Pickering emulsions, variable amounts of hydroxypropylcellulose (HPC) were added in order to study its effects on the colloidal behavior of the system.<sup>[197]</sup> In particular, the presence of the biopolymer enhances the colloidal stability of the Pickering emulsions by hindering their collision and aggregation due to the increase of viscosity and to the decrease of the surface tension in water. The solvent casting method was carried out to prepare very homogeneous nanocomposites displaying the wax/HNTs microparticles embedded in the cellulosic matrix. Herein, wettability studies suggested that the films hydrophobicity increased with the increasing amount

of paraffin/halloysite microparticles and, more interestingly, the rolling process of water droplets on the surface is facilitated. This feature is important especially for applications as protective coatings because it endows an efficient removal of other species from the treated material. Also, the addition of microparticles is responsible for the decrease of the vapor permeability of the nanocomposites, which can act as a gas barrier. Studies on the transparency and colorimetric properties of the films suggested that they can be tuned by changing the amount of the wax/HNTs microparticles in the polymeric matrix. The thermal properties were also investigated and it was found that the prepared nanocomposites can work as a heat reservoirs better than pure HPC due to the presence of paraffin. All these properties make the HPC/wax/halloysite promising for application as packaging materials and/or for the treatment of cultural heritage.<sup>[197]</sup> Indeed, spraying this formulation on the surface of a hydraulic mortar allowed to obtain a protective hydrophobic coating on the stone, without affecting its overall macroscopic aspect and colorimetric features.<sup>[198]</sup>

a)



b)

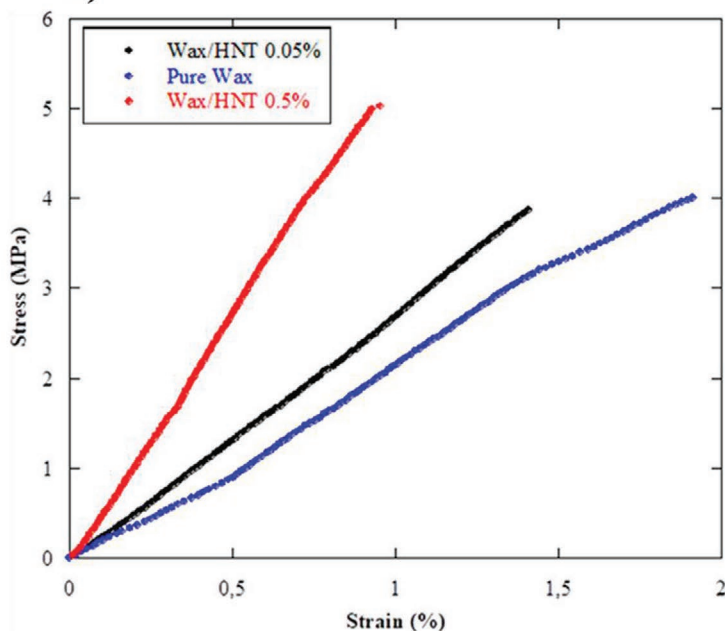


**Figure 19.** a) Optical photos of the waterlogged archeological wood before (up) and after (down) consolidation with wax/HNTs Pickering emulsions. The scale bars are 1 cm. b) Stress versus strain curves for archeological wood consolidated with pure wax, wax/HNTs 0.05% w/w, and wax/HNTs 0.5% w/w Pickering emulsions. Reproduced with permission.<sup>[196]</sup> Copyright 2021, American Chemical Society.

## 5. Conclusions and Perspectives

Pickering emulsions have received increasing attention in the recent times due to their easy processing, manageability and great potential in a wide range of applications. As reported in the first paragraphs of this work, the colloidal stability of Pickering emulsions is crucial and it depends by many parameters such as the nature and wettability of the solid stabilizing particles, their morphology and concentration, the chemical nature of the oil phase, the water/oil ratio, viscosity, pH and ionic strength of the environment, As a consequence, the physico-chemical properties of the system (i.e., droplets size, rheology, stability) can be tailored.

For what concerns the interfacially active solids, a very broad class of materials can be exploited for this purpose, and they can have both organic and inorganic nature. Proteins, polysaccharides, food-grade products, cellulosic derivatives, polymers and carbon based particles are a few examples of the former class. Gold nanoparticles, titania, magnetite, nanoceria, silica, and nanoclays, instead, are some inorganic

counterparts. Among clays, Halloysite Nanotubes hold a certain importance.

Owing to its peculiar hollow nanotubular morphology, surface charges, aspect ratio, eco-friendliness, biocompatibility and low cost, halloysite is an excellent material for the stabilization of Pickering emulsions, as demonstrated by several volumes in literature.

The adsorption of the clay particles at the liquid/liquid interface, together with the existence of capillary interactions between the tubes, provides steric hindrance to the droplets and it prevents any collision, aggregation and phase separation.

This review discussed about these aspects in detail and also enlightened the different fields where these particles can be proficiently exploited. The environmental applications, consisting of either oil spill (bio-)remediation or removal of polluting chemicals from water has largely benefited from use of halloysite based Pickering emulsions. Also, catalysis, drug delivery and cultural heritage treatment represent other areas of research and technology where the impact of halloysite



stabilized Pickering emulsions has been strong. Undoubtedly, being a quite new and open field, the research has not ceased.

New investigation routes are being taken and they deal with the use of solids of mixed nature or binary particles for the co-stabilization of droplets by joining together their proper features (charges, morphologies, chemistry, wettability, etc.) to create some emerging synergistic effects and to endow Pickering emulsions with different functionalities. Also, the development of multi-compartmented systems can be investigated to create water-in-oil-in-water (w/o/w) or oil-in-water-in-oil (o/w/o) double emulsions. In addition, halloysite stabilized Pickering emulsions could also be exploited for the preparation of Janus Nanotubes, which would be asymmetric particles bearing different functionalities on the two opposites sides of a single nanotube, thus opening the way to a new class of materials, which has not still been reported in literature.

## Acknowledgements

The authors acknowledge the University of Palermo for financial support.

Open Access Funding provided by Università degli Studi di Palermo within the CRUI-CARE Agreement.

## Conflict of Interest

The authors declare no conflict of interest.

## Keywords

catalysis, cultural heritage, environment, halloysite nanotubes, health applications, nanoclays, Pickering emulsions

Received: November 30, 2021

Revised: December 23, 2021

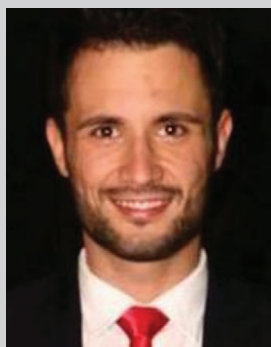
Published online: February 5, 2022

- [1] S. U. Pickering, *J. Chem. Soc. Trans.* **1907**, 91, 2001.  
 [2] W. Ramsden, *Proc. R. Soc. London* **1904**, 72, 156.  
 [3] M. Destribats, M. Rouvet, C. Gehin-Delval, C. Schmitt, B. P. Binks, *Soft Matter* **2014**, 10, 6941.  
 [4] S. Arditty, C. P. Whitby, B. P. Binks, V. Schmitt, F. Leal-Calderon, *Eur. Phys. J. E* **2003**, 11, 273.  
 [5] J. Frelichowska, M.-A. Bolzinger, J. Pelletier, J.-P. Valour, Y. Chevalier, *Int. J. Pharm.* **2009**, 371, 56.  
 [6] H. Jiang, Y. Sheng, T. Ngai, *Curr. Opin. Colloid Interface Sci.* **2020**, 49, 1.  
 [7] M. Dinkgreve, K. P. Velikov, D. Bonn, *Phys. Chem. Chem. Phys.* **2016**, 18, 22973.  
 [8] W. J. Ganley, J. S. van Duijneveldt, *Langmuir* **2017**, 33, 1679.  
 [9] V. Calabrese, J. C. Courtenay, K. J. Edler, J. L. Scott, *Curr. Opin. Green Sustainable Chem.* **2018**, 12, 83.  
 [10] B. P. Binks, *Curr. Opin. Colloid Interface Sci.* **2002**, 7, 21.  
 [11] J. Wu, G.-H. Ma, *Small* **2016**, 12, 4633.  
 [12] D. Marku, M. Wahlgren, M. Rayner, M. Sjö, A. Timgren, *Int. J. Pharm.* **2012**, 428, 1.  
 [13] T. Sharma, N. Velmurugan, P. Patel, B. H. Chon, J. S. Sangwai, *Pet. Sci. Technol.* **2015**, 33, 1595.  
 [14] L. E. Low, S. P. Siva, Y. K. Ho, E. S. Chan, B. T. Tey, *Adv. Colloid Interface Sci.* **2020**, 277, 102117.  
 [15] B. P. Binks, S. O. Lumsden, *Langmuir* **2000**, 16, 8622.  
 [16] T. Xu, J. Yang, S. Hua, Y. Hong, Z. Gu, L. Cheng, Z. Li, C. Li, *Trends Food Sci. Technol.* **2020**, 105, 334.  
 [17] G. Kaptay, *Colloids Surf., A* **2006**, 282–283, 387.  
 [18] C. Li, Y. Li, P. Sun, C. Yang, *Colloids Surf., A* **2013**, 431, 142.  
 [19] S. Varanasi, L. Henzel, L. Mendoza, R. Prathapan, W. Batchelor, R. Tabor, G. Garnier, *Front. Chem.* **2018**, 6, 409.  
 [20] D. E. Tambe, M. M. Sharma, *Adv. Colloid Interface Sci.* **1994**, 52, 1.  
 [21] J. P. E. Machado, R. A. de Freitas, F. Wypych, *Appl. Clay Sci.* **2019**, 169, 10.  
 [22] Y. Chevalier, M.-A. Bolzinger, *Colloids Surf., A* **2013**, 439, 23.  
 [23] N. P. Ashby, B. P. Binks, *Phys. Chem. Chem. Phys.* **2000**, 2, 5640.  
 [24] R. Aveyard, B. P. Binks, J. H. Clint, *Adv. Colloid Interface Sci.* **2003**, 100–102, 503.  
 [25] P. A. Kralchevsky, N. D. Denkov, *Curr. Opin. Colloid Interface Sci.* **2001**, 6, 383.  
 [26] P. A. Kralchevsky, K. Nagayama, *Adv. Colloid Interface Sci.* **2000**, 85, 145.  
 [27] B. R. Midmore, *Colloids Surf., A* **1998**, 132, 257.  
 [28] P. Lv, D. Wang, Y. Chen, S. Zhu, J. Zhang, L. Mao, Y. Gao, F. Yuan, *Food Hydrocoll.* **2020**, 108, 105992.  
 [29] B. P. Binks, J. A. Rodrigues, *Langmuir* **2007**, 23, 7436.  
 [30] Abdullah, J. Weiss, T. Ahmad, C. Zhang, H. Zhang, *Trends Food Sci. Technol.* **2020**, 106, 91.  
 [31] J. Lu, W. Zhou, J. Chen, Y. Jin, K. B. Walters, S. Ding, *RSC Adv.* **2015**, 5, 9416.  
 [32] R. Chanamai, G. Horn, D. J. McClements, *J. Colloid Interface Sci.* **2002**, 247, 167.  
 [33] M. El-Mahrab-Robert, V. Rosilio, M.-A. Bolzinger, P. Chaminade, J.-L. Grossiord, *Int. J. Pharm.* **2008**, 348, 89.  
 [34] M. V. Tzoumaki, T. Moschakis, V. Kiosseoglou, C. G. Biliaderis, *Food Hydrocoll.* **2011**, 25, 1521.  
 [35] Z. Yang, W. Wang, G. Wang, X. Tai, *Colloids Surf. Physicochem. Eng. Asp.* **2020**, 585, 124098.  
 [36] S. Komatsu, Y. Ikeda, T.-A. Asoh, R. Ishihara, A. Kikuchi, *Langmuir* **2018**, 34, 3981.  
 [37] N. Fessi, M. F. Nsib, Y. Chevalier, C. Guillard, F. Dappozze, A. Houas, L. Palmisano, F. Parrino, *Langmuir* **2019**, 35, 2129.  
 [38] C.-Y. Xie, S.-X. Meng, L.-H. Xue, R.-X. Bai, X. Yang, Y. Wang, Z.-P. Qiu, B. P. Binks, T. Guo, T. Meng, *Langmuir* **2017**, 33, 14139.  
 [39] N. Sun, Q. Li, D. Luo, P. Sui, Q. Jiang, J. Liu, A. Li, W. Si, Y. Ma, *Colloids Surf., A* **2021**, 608, 125588.  
 [40] I. Martín-Fabiani, M. L. Koh, F. Dalmas, K. L. Elidottir, S. J. Hinder, I. Jurewicz, M. Lansalot, E. Bourgeat-Lami, J. L. Keddie, *ACS Appl. Nano Mater.* **2018**, 1, 3956.  
 [41] D. Liu, F. Zhou, C. Li, T. Zhang, H. Zhang, W. Cai, Y. Li, *Angew. Chem., Int. Ed.* **2015**, 54, 9596.  
 [42] S. Levine, B. D. Bowen, S. J. Partridge, *Colloids Surf.* **1989**, 38, 325.  
 [43] F. Xue, Y. Zhang, F. Zhang, X. Ren, H. Yang, *ACS Appl. Mater. Interfaces* **2017**, 9, 8403.  
 [44] B. P. Binks, D. Yin, *Soft Matter* **2016**, 12, 6858.  
 [45] H. Jiang, L. Hong, Y. Li, T. Ngai, *Angew. Chem., Int. Ed.* **2018**, 57, 11662.  
 [46] Y. Li, J. Liu, X. He, D. Kong, C. Zhou, H. Wu, Z. Yang, Z. Yang, Y. Hu, *Macromol. Mater. Eng.* **2020**, 305, 1900851.  
 [47] A. Shi, X. Feng, Q. Wang, B. Adhikari, *Food Hydrocoll.* **2020**, 109, 106117.  
 [48] Z. Gao, J. Zhao, Y. Huang, X. Yao, K. Zhang, Y. Fang, K. Nishinari, G. O. Phillips, F. Jiang, H. Yang, *LWT – Food Sci. Technol.* **2017**, 76, 1.  
 [49] F. Liu, C.-H. Tang, *Food Hydrocoll.* **2016**, 60, 606.  
 [50] M. Sarker, N. Tomczak, S. Lim, *ACS Appl. Mater. Interfaces* **2017**, 9, 11193.  
 [51] A. Can Karaca, M. T. Nickerson, N. H. Low, *J. Agric. Food Chem.* **2011**, 59, 13203.

- [52] Y. Zou, C. van Baalen, X. Yang, E. Scholten, *Food Hydrocoll.* **2018**, 80, 130.
- [53] Y. Zhu, X. Luo, X. Wu, W. Li, B. Li, A. Lu, S. Liu, *Cellulose* **2017**, 24, 207.
- [54] S. Ge, L. Xiong, M. Li, J. Liu, J. Yang, R. Chang, C. Liang, Q. Sun, *Food Chem.* **2017**, 234, 339.
- [55] M. Sjöö, S. C. Emek, T. Hall, M. Rayner, M. Wahlgren, *J. Colloid Interface Sci.* **2015**, 450, 182.
- [56] Q. Jiang, S. Li, L. Du, Y. Liu, Z. Meng, *J. Colloid Interface Sci.* **2021**, 602, 822.
- [57] Y. Lu, J. Li, L. Ge, W. Xie, D. Wu, *Carbohydr. Polym.* **2021**, 255, 117483.
- [58] J. C. Courtenay, Y. Jin, J. Schmitt, K. M. Z. Hossain, N. Mahmoudi, K. J. Edler, J. L. Scott, *Langmuir* **2021**, 37, 6864.
- [59] J. Shin, S.-M. Seo, I.-K. Park, J. Hyun, *Carbohydr. Polym.* **2021**, 254, 117381.
- [60] F. Laredj-Bouezg, M.-A. Bolzinger, J. Pelletier, Y. Chevalier, *Int. J. Pharm.* **2017**, 531, 134.
- [61] J.-P. Douliez, N. Martin, T. Beneyton, J.-C. Eloi, J.-P. Chapel, L. Navailles, J.-C. Baret, S. Mann, L. Béven, *Angew. Chem., Int. Ed.* **2018**, 57, 7780.
- [62] H. Chen, E. M. Nofen, K. Rykaczewski, L. L. Dai, *J. Colloid Interface Sci.* **2017**, 504, 440.
- [63] X. Mi, X. Wang, C. Gao, W. Su, Y. Zhang, X. Tan, J. Gao, Y. Liu, *J. Mater. Sci.* **2020**, 55, 1946.
- [64] X. Zhai, J. Gao, X. Wang, S. Mei, R. Zhao, Y. Wu, C. Hao, J. Yang, Y. Liu, *Chem. Eng. J.* **2018**, 345, 209.
- [65] N. M. Briggs, J. S. Weston, B. Li, D. Venkataramani, C. P. Aichele, J. H. Harwell, S. P. Crossley, *Langmuir* **2015**, 31, 13077.
- [66] C. C. Berton-Carabin, K. Schroën, *Annu. Rev. Food Sci. Technol.* **2015**, 6, 263.
- [67] M. Calabi-Floody, B. Theng, M. L. Mora, *Clay Miner. – CLAY Min.* **2009**, 44, 161.
- [68] F. Uddin, *Metall. Mater. Trans. A* **2008**, 39, 2804.
- [69] S. Guillot, F. Bergaya, C. de Azevedo, F. Warmont, J.-F. Tranchant, *J. Colloid Interface Sci.* **2009**, 333, 563.
- [70] Y. Cui, M. Threlfall, J. S. van Duijneveldt, *J. Colloid Interface Sci.* **2011**, 356, 665.
- [71] L. G. Torres, R. Iturbe, M. J. Snowden, B. Z. Chowdhry, S. A. Leharne, *Colloids Surf., A* **2007**, 302, 439.
- [72] C. H. Zhou, J. Keeling, *Appl. Clay Sci.* **2013**, 74, 3.
- [73] M. Vis, J. Opdam, I. S. J. van 't Oor, G. Soligno, R. van Roij, R. H. Tromp, B. H. Erné, *ACS Macro Lett.* **2015**, 4, 965.
- [74] K. R. Peddiredy, T. Nicolai, L. Benyahia, I. Capron, *ACS Macro Lett.* **2016**, 5, 283.
- [75] N. Ballard, A. D. Law, S. A. F. Bon, *Soft Matter* **2019**, 15, 1186.
- [76] T. Lu, H. Gou, H. Rao, G. Zhao, *J. Environ. Chem. Eng.* **2021**, 9, 105941.
- [77] J. Wang, H. Deng, Y. Sun, C. Yang, *J. Colloid Interface Sci.* **2020**, 562, 529.
- [78] Q. Li, Q. Mao, C. Yang, S. Zhang, G. He, X. Zhang, W. Zhang, *Int. J. Biol. Macromol.* **2019**, 141, 987.
- [79] T. Lu, Y. Zhu, W. Wang, A. Wang, *J. Cleaner Prod.* **2020**, 277, 124092.
- [80] F. Pignon, A. Magnin, J.-M. Piau, *J. Rheol.* **1998**, 42, 1349.
- [81] C. P. Whitby, P. C. Garcia, *Appl. Clay Sci.* **2014**, 96, 56.
- [82] D. Yu, G. Li, F. Kong, H. Wang, W. Liu, Z. Song, X. Meng, J. R. H. Zhao, *Appl. Clay Sci.* **2020**, 191, 105608.
- [83] J. Shin, J. Park, H. Kim, *Appl. Clay Sci.* **2019**, 182, 105288.
- [84] R. da Silva, T. Kuczera, G. Picheth, L. Menezes, F. Wypych, R. A. de Freitas, *J. Dispersion Sci. Technol.* **2018**, 39, 901.
- [85] T. Nallamilli, M. G. Basavaraj, *Appl. Clay Sci.* **2017**, 148, 68.
- [86] J. Tully, R. Yendluri, Y. Lvov, *Biomacromolecules* **2016**, 17, 615.
- [87] F. Ferrante, N. Armata, G. Cavallaro, G. Lazzara, *J. Phys. Chem. C* **2017**, 121, 2951.
- [88] E. Joussein, S. Petit, G. J. Churchman, B. Theng, D. Righi, B. Delvaux, *Clay Miner.* **2005**, 40, 383.
- [89] G. Cavallaro, S. Milioto, S. Konnova, G. Fakhru'llina, F. Akhatova, G. Lazzara, R. Fakhru'llin, Y. Lvov, *ACS Appl. Mater. Interfaces* **2020**, 12, 24348.
- [90] Y. M. Lvov, D. G. Shchukin, H. Mohwald, R. R. Price, *ACS Nano* **2008**, 2, 814.
- [91] M. Du, B. Guo, D. Jia, *Polym. Int.* **2010**, 59, 574.
- [92] G. Cavallaro, L. Chiappisi, P. Pasbakhsh, M. Gradzielski, G. Lazzara, *Appl. Clay Sci.* **2018**, 160, 71.
- [93] J. González-Rivera, A. Spepi, C. Ferrari, I. Longo, J. T. Rodriguez, E. Fantechi, C. Innocenti, F. Pineider, M. A. Vera-Ramírez, M. R. Tiné, C. Duce, *Appl. Clay Sci.* **2020**, 196, 105752.
- [94] E. Abdullayev, A. Joshi, W. Wei, Y. Zhao, Y. Lvov, *ACS Nano* **2012**, 6, 7216.
- [95] L. Lisuzzo, B. Wicklein, G. L. Dico, G. Lazzara, G. del Real, P. Aranda, E. Ruiz-Hitzky, *Dalton Trans.* **2020**, 49, 3830.
- [96] H. Zhang, C. Cheng, H. Song, L. Bai, Y. Cheng, X. Ba, Y. Wu, *Chem. Commun.* **2019**, 55, 1040.
- [97] G. Cavallaro, G. Lazzara, S. Milioto, *J. Phys. Chem. C* **2012**, 116, 21932.
- [98] B. V. Derjaguin, L. D. Landau, *Acta Physicochim. URSS* **1941**, 14, 733.
- [99] L. Lisuzzo, G. Cavallaro, S. Milioto, G. Lazzara, *J. Colloid Interface Sci.* **2022**, 608, 424.
- [100] G. Cavallaro, G. Lazzara, S. Milioto, F. Parisi, *Langmuir* **2015**, 31, 7472.
- [101] L. Lisuzzo, G. Cavallaro, F. Parisi, S. Milioto, G. Lazzara, *Ceram. Int.* **2019**, 45, 2858.
- [102] B. Huang, M. Liu, C. Zhou, *Cellulose* **2017**, 24, 2861.
- [103] P. Pasbakhsh, G. J. Churchman, J. L. Keeling, *Appl. Clay Sci.* **2013**, 74, 47.
- [104] G. I. Fakhru'llina, F. S. Akhatova, Y. M. Lvov, R. F. Fakhru'llin, *Environ. Sci. Nano* **2015**, 2, 54.
- [105] M. Kryuchkova, A. Danilushkina, Y. Lvov, R. Fakhru'llin, *Environ. Sci. Nano* **2016**, 3, 442.
- [106] C. Duce, S. Vecchio Cipriotti, L. Ghezzi, V. Ierardi, M. Tiné, *J. Therm. Anal. Calorim.* **2015**, 121, 1011.
- [107] A. Spepi, C. Duce, A. Pedone, D. Presti, J.-G. Rivera, V. Ierardi, M. R. Tiné, *J. Phys. Chem. C* **2016**, 120, 26759.
- [108] B. Huang, M. Liu, C. Zhou, *Carbohydr. Polym.* **2017**, 175, 689.
- [109] G. Gorrasi, R. Pantani, M. Murariu, P. Dubois, *Macromol. Mater. Eng.* **2014**, 299, 104.
- [110] E. Abdullayev, Y. Lvov, *J. Mater. Chem. B* **2013**, 1, 2894.
- [111] Y. Lvov, W. Wang, L. Zhang, R. Fakhru'llin, *Adv. Mater.* **2016**, 28, 1227.
- [112] G. Gorrasi, *Carbohydr. Polym.* **2015**, 127, 47.
- [113] J. Ouyang, B. Guo, L. Fu, H. Yang, Y. Hu, A. Tang, H. Long, Y. Jin, J. Chen, J. Jiang, *Mater. Des.* **2016**, 110, 169.
- [114] L. Fan, B. Li, Q. Wang, A. Wang, J. Zhang, *Adv. Mater. Interfaces* **2014**, 1, 1300136.
- [115] R. R. Price, B. P. Gaber, Y. Lvov, *J. Microencapsul.* **2001**, 18, 713.
- [116] D. G. Shchukin, S. V. Lamaka, K. A. Yasakau, M. L. Zheludkevich, M. G. S. Ferreira, H. Mohwald, *J. Phys. Chem. C* **2008**, 112, 958.
- [117] L. Lisuzzo, G. Cavallaro, P. Pasbakhsh, S. Milioto, G. Lazzara, *J. Colloid Interface Sci.* **2019**, 547, 361.
- [118] L. Lisuzzo, G. Cavallaro, S. Milioto, G. Lazzara, *J. Nanostructure Chem.* **2021**, 11, 663.
- [119] M. R. Dzamukova, E. A. Naumenko, Y. M. Lvov, R. F. Fakhru'llin, *Sci. Rep.* **2015**, 5, 10560.
- [120] M. T. Viseras, C. Aguzzi, P. Cerezo, C. Viseras, C. Valenzuela, *Microporous Mesoporous Mater.* **2008**, 108, 112.
- [121] C. Aguzzi, C. Viseras, P. Cerezo, I. Salcedo, R. Sánchez-Espejo, C. Valenzuela, *Colloids Surf., B* **2013**, 105, 75.
- [122] V. Bugatti, G. Viscusi, C. Naddeo, G. Gorrasi, *Nanomaterials* **2017**, 7, 213.
- [123] M. Makaremi, P. Pasbakhsh, G. Cavallaro, G. Lazzara, Y. K. Aw, S. M. Lee, S. Milioto, *ACS Appl. Mater. Interfaces* **2017**, 9, 17476.

- [124] I. L. Hia, W. H. Lam, S.-P. Chai, E.-S. Chan, P. Pasbakhsh, *Mater. Chem. Phys.* **2018**, 215, 69.
- [125] E. Abdullayev, Y. Lvov, *J. Mater. Chem.* **2010**, 20, 6681.
- [126] J.-P. Wang, X. Song, J.-K. Wang, X. Cui, Q. Zhou, T. Qi, G. L. Li, *Adv. Mater. Interfaces* **2019**, 6, 1900055.
- [127] S. Sadjadi, *Appl. Clay Sci.* **2020**, 189, 105537.
- [128] Y. Zhao, S. Thapa, L. Weiss, Y. Lvov, *Adv. Eng. Mater.* **2014**, 16, 1391.
- [129] F. Liu, L. Bai, H. Zhang, H. Song, L. Hu, Y. Wu, X. Ba, *ACS Appl. Mater. Interfaces* **2017**, 9, 31626.
- [130] M. Liu, C. Wu, Y. Jiao, S. Xiong, C. Zhou, *J. Mater. Chem. B* **2013**, 1, 2078.
- [131] T. T. Haw, F. Hart, A. Rashidi, P. Pasbakhsh, *Appl. Clay Sci.* **2020**, 188, 105533.
- [132] H. Zhang, T. Ren, Y. Ji, L. Han, Y. Wu, H. Song, L. Bai, X. Ba, *ACS Appl. Mater. Interfaces* **2015**, 7, 23805.
- [133] Y. Zhao, W. Kong, Z. Jin, Y. Fu, W. Wang, Y. Zhang, J. Liu, B. Zhang, *Appl. Energy* **2018**, 222, 180.
- [134] W. Ma, Y. Higaki, A. Takahara, *Adv. Mater. Interfaces* **2017**, 4, 1700907.
- [135] F. Wu, K. Pickett, A. Panchal, M. Liu, Y. Lvov, *ACS Appl. Mater. Interfaces* **2019**, 11, 25445.
- [136] K. Feng, G.-Y. Hung, J. Liu, M. Li, C. Zhou, M. Liu, *Chem. Eng. J.* **2018**, 331, 744.
- [137] O. Owoseni, E. Nyankson, Y. Zhang, S. J. Adams, J. He, G. L. McPherson, A. Bose, R. B. Gupta, V. T. John, *Langmuir* **2014**, 30, 13533.
- [138] E. Abdullayev, R. Price, D. Shchukin, Y. Lvov, *ACS Appl. Mater. Interfaces* **2009**, 1, 1437.
- [139] A. Saha, A. Nikova, P. Venkataraman, V. T. John, A. Bose, *ACS Appl. Mater. Interfaces* **2013**, 5, 3094.
- [140] E. P. Lewandowski, P. C. Searson, K. J. Stebe, *J. Phys. Chem. B* **2006**, 110, 4283.
- [141] J.-B. Fournier, P. Galatola, *Phys. Rev. E* **2002**, 65, 031601.
- [142] J. C. Loudet, A. M. Alsayed, J. Zhang, A. G. Yodh, *Phys. Rev. Lett.* **2005**, 94, 018301.
- [143] D. Kpogbemabou, G. Lecomte-Nana, A. Aimable, M. Bienia, V. Niknam, C. Carrion, *Colloids Surf., A* **2014**, 463, 85.
- [144] X. Cai, C. Li, Q. Tang, B. Zhen, X. Xie, W. Zhu, C. Zhou, L. Wang, *Appl. Clay Sci.* **2019**, 172, 115.
- [145] J. Frelichowska, M.-A. Bolzinger, Y. Chevalier, *Colloids Surf., A* **2009**, 343, 70.
- [146] P. Sadeh, I. Najafipour, M. Gholami, *Colloids Surf., A* **2019**, 577, 231.
- [147] M. Ouadaker, X. Jiang, P. Bowen, M. Bienia, C. Pagnoux, A. Aimable, *Colloids Surf., A* **2020**, 585, 124156.
- [148] M. Donnet, P. Bowen, J. Lemaître, *J. Colloid Interface Sci.* **2009**, 340, 218.
- [149] K. Buruga, J. T. Kalathi, *J. Polym. Res.* **2019**, 26, 210.
- [150] D. Stehl, T. Skale, L. Hohl, Y. Lvov, J. Koetz, M. Kraume, A. Drews, R. von Klitzing, *ACS Appl. Nano Mater.* **2020**, 3, 11743.
- [151] B. Ates, S. Koytepe, A. Ulu, C. Gurses, V. K. Thakur, *Chem. Rev.* **2020**, 120, 9304.
- [152] R. M. Atlas, T. C. Hazen, *Environ. Sci. Technol.* **2011**, 45, 6709.
- [153] B. D. Goldstein, H. J. Osofsky, M. Y. Lichtveld, *N. Engl. J. Med.* **2011**, 364, 1334.
- [154] S. E. Allan, B. W. Smith, K. A. Anderson, *Environ. Sci. Technol.* **2012**, 46, 2033.
- [155] R. R. Lessard, G. DeMarco, *Spill Sci. Technol. Bull.* **2000**, 6, 59.
- [156] J. Fu, Y. Gong, X. Zhao, S. E. O'Reilly, D. Zhao, *Environ. Sci. Technol.* **2014**, 48, 14392.
- [157] P. Venkataraman, J. Tang, E. Frenkel, G. L. McPherson, J. He, S. R. Raghavan, V. Kolesnichenko, A. Bose, V. T. John, *ACS Appl. Mater. Interfaces* **2013**, 5, 3572.
- [158] D. E. Tambe, M. M. Sharma, *J. Colloid Interface Sci.* **1993**, 157, 244.
- [159] J. C. Athas, K. Jun, C. McCafferty, O. Owoseni, V. T. John, S. R. Raghavan, *Langmuir* **2014**, 30, 9285.
- [160] O. F. Ojo, A. Farinmade, J. Trout, M. Omarova, J. He, V. John, D. A. Blake, Y. M. Lvov, D. Zhang, D. Nguyen, A. Bose, *ACS Appl. Nano Mater.* **2019**, 2, 3490.
- [161] A. Farinmade, O. F. Ojo, J. Trout, J. He, V. John, D. A. Blake, Y. M. Lvov, D. Zhang, D. Nguyen, A. Bose, *ACS Appl. Mater. Interfaces* **2020**, 12, 1840.
- [162] Z. Li, K. Lee, T. King, M. C. Boufadel, A. D. Venosa, *Mar. Pollut. Bull.* **2009**, 58, 735.
- [163] N. E. Kimes, A. V. Callaghan, J. M. Suflita, P. J. Morris, *Front. Microbiol.* **2014**, 5, 603.
- [164] T. Yu, L. T. Swientoniewski, M. Omarova, M.-C. Li, I. I. Negulescu, N. Jiang, O. A. Darvish, A. Panchal, D. A. Blake, Q. Wu, Y. M. Lvov, V. T. John, D. Zhang, *ACS Appl. Mater. Interfaces* **2019**, 11, 27944.
- [165] C. Fetsch, S. Flecks, D. Gieseler, C. Marschelke, J. Ulbricht, K.-H. van Pée, R. Luxenhofer, *Macromol. Chem. Phys.* **2015**, 216, 547.
- [166] A. Panchal, L. T. Swientoniewski, M. Omarova, T. Yu, D. Zhang, D. A. Blake, V. John, Y. M. Lvov, *Colloids Surf., B* **2018**, 164, 27.
- [167] A. Panchal, N. Rahman, S. Konnova, R. Fakhruddin, D. Zhang, D. Blake, V. John, E. Ivanov, Y. Lvov, *ACS Appl. Nano Mater.* **2020**, 3, 1263.
- [168] A. Eskhan, F. Banat, M. Abu Haija, S. Al-Asheh, *Langmuir* **2019**, 35, 2343.
- [169] C. Zhou, H. Li, H. Zhou, H. Wang, P. Yang, S. Zhong, *J. Sep. Sci.* **2015**, 38, 1365.
- [170] G. Wulff, *Chem. Rev.* **2002**, 102, 1.
- [171] T. Zhao, J. Chen, Y. Chen, Y. Zhang, J. Peng, *J. Dispersion Sci. Technol.* **2021**, 42, 934.
- [172] B. Hentschel, G. Kiedorf, M. Gerlach, C. Hamel, A. Seidel-Morgenstern, H. Freund, K. Sundmacher, *Ind. Eng. Chem. Res.* **2015**, 54, 1755.
- [173] R. von Klitzing, D. Stehl, T. Pogrzeba, R. Schomäcker, R. Minullina, A. Panchal, S. Konnova, R. Fakhruddin, J. Koetz, H. Möhwald, Y. Lvov, *Adv. Mater. Interfaces* **2016**, 4, 1600435.
- [174] D. Stehl, N. Milojević, S. Stock, R. Schomäcker, R. von Klitzing, *Ind. Eng. Chem. Res.* **2019**, 58, 2524.
- [175] W. Guan, Y. Zhang, Y. Wei, B. Li, Y. Feng, C. Yan, P. Huo, Y. Yan, *Fuel* **2020**, 278, 118362.
- [176] X.-N. Huang, F.-Z. Zhou, T. Yang, S.-W. Yin, C.-H. Tang, X.-Q. Yang, *Food Hydrocoll.* **2019**, 93, 34.
- [177] Z. Gao, R. Xie, G. Fan, L. Yang, F. Li, *ACS Sustainable Chem. Eng.* **2017**, 5, 5852.
- [178] C. V. Nguyen, Y.-T. Liao, T.-C. Kang, J. E. Chen, T. Yoshikawa, Y. Nakasaka, T. Masuda, K. C.-W. Wu, *Green Chem.* **2016**, 18, 5957.
- [179] A. Aijaz, J. Masa, C. Rösler, W. Xia, P. Weide, A. J. R. Botz, R. A. Fischer, W. Schuhmann, M. Muhler, *Angew. Chem., Int. Ed.* **2016**, 55, 4087.
- [180] Y. Chen, W. Guan, Y. Zhang, C. Yan, B. Li, Y. Wei, J. Pan, Y. Yan, *Energy Fuels* **2020**, 34, 14264.
- [181] Z. Wei, C. Wang, H. Liu, S. Zou, Z. Tong, *J. Appl. Polym. Sci.* **2012**, 125, E358.
- [182] K. Rezwan, Q. Z. Chen, J. J. Blaker, A. R. Boccaccini, *Biomaterials* **2006**, 27, 3413.
- [183] Y. Hu, S. Liu, X. Li, T. Yuan, X. Zou, Y. He, X. Dong, W. Zhou, Z. Yang, *J. Mater. Sci.* **2018**, 53, 14774.
- [184] L.-Y. Li, Y.-M. Zhou, R.-Y. Gao, X.-C. Liu, H.-H. Du, J.-L. Zhang, X.-C. Ai, J.-P. Zhang, L.-M. Fu, L. H. Skibsted, *Biomaterials* **2019**, 190–191, 86.
- [185] V. Shanmugam, S. Selvakumar, C.-S. Yeh, *Chem. Soc. Rev.* **2014**, 43, 6254.
- [186] R. Gagliano Candela, F. Maggi, G. Lazzara, S. Rosselli, M. Bruno, *Plants* **2019**, 8, 300.
- [187] G. Cavallaro, S. Milioto, L. Nigamatzyanova, F. Akhatova, R. Fakhruddin, G. Lazzara, *ACS Appl. Nano Mater.* **2019**, 2, 3169.
- [188] S. Barreca, M. Bruno, L. Oddo, S. Orecchio, *Nat. Prod. Res.* **2019**, 33, 947.

- [189] X. Yang, J. Cai, L. Chen, X. Cao, H. Liu, M. Liu, *Chem. Eng. J.* **2021**, 425, 130623.
- [190] T. D. Bugg, M. Ahmad, E. M. Hardiman, R. Singh, *Curr. Opin. Biotechnol.* **2011**, 22, 394.
- [191] P. Hoffmann, *Holzforschung* **2010**, 64, 725.
- [192] J. Kowalczyk, A. Rachocki, M. Broda, B. Mazela, G. A. Ormondroyd, J. Tritt-Goc, *Wood Sci. Technol.* **2019**, 53, 1207.
- [193] M. Sandström, F. Jalilehvand, I. Persson, U. Gelius, P. Frank, I. Hall-Roth, *Nature* **2002**, 415, 893.
- [194] Z. Walsh, E.-R. Janeček, M. Jones, O. A. Scherman, *Stud. Conserv.* **2017**, 62, 173.
- [195] M. Christensen, H. Kutzke, F. K. Hansen, *Wood Sci. Conserv.* **2012**, 13, S183.
- [196] L. Lisuzzo, T. Hueckel, G. Cavallaro, S. Sacanna, G. Lazzara, *ACS Appl. Mater. Interfaces* **2021**, 13, 1651.
- [197] L. Lisuzzo, M. R. Caruso, G. Cavallaro, S. Milioto, G. Lazzara, *Ind. Eng. Chem. Res.* **2021**, 60, 1656.
- [198] M. R. Caruso, B. Megna, L. Lisuzzo, G. Cavallaro, S. Milioto, G. Lazzara, *J. Coat. Technol. Res.* **2021**, 18, 1625.



**Lorenzo Lisuzzo** is Assistant Professor at the Department of Physics and Chemistry, University of Palermo (Italy). He was Visiting Student Researcher at the Molecular Design Institute – Department of Chemistry of the New York University (USA) as Fulbright Alumnus. His research interests focus on the design of eco-sustainable functional biohybrid materials and on catalysis as well. He is author of more than 20 publications in peer-reviewed international journals.



**Giuseppe Cavallaro** is assistant professor at the Department of Physics and Chemistry, University of Palermo, Italy. He was Research Associate at Institute of Micromanufacturing, Louisiana Tech University, (USA) and Institut für Chemie, Technische Universität Berlin (Germany). His research activities focus on nanoclays and polymer/nanoparticle interactions. He is author of more than 110 publications in peer-reviewed international journals.



**Stefana Milioto** is Full Professor in Physical-Chemistry at the Department of Physics and Chemistry of the University of Palermo. Scientific interest deals with the physico-chemical studies of self-assembled structures as well as inorganic nanoparticles for application in the field of Cultural Heritage, drug delivery, and environment. She has more than 170 publications in peer-reviewed international journals.



**Giuseppe Lazzara** is full professor in Chemistry for environment and cultural heritage at the Department of Physics and Chemistry, University of Palermo, Italy. He received his Ph.D. degree in Chemistry in 2007. He was Postdoc at the Chemistry Department, Lund University (Sweden). He is involved in several projects on halloysite clay nanotubes for conservation of cultural heritage. Lazzara has more than 190 publications in peer-reviewed international journals, an edited book and 2 patents in the field of nanomaterials for cultural heritage.